UNIVERSITÄTSKLINIKUM HAMBURG-EPPENDORF

Zentrum für Experimentelle Medizin

Institut für Biochemie und Signaltransduktion

Direktor: Prof. Dr. rer. nat. Aymelt Itzen

Functional role of fatty acid synthase for signal transduction in human acute myeloid leukemia cells

Dissertation

zur Erlangung des Grades eines Doktors der Medizin

an der Medizinischen Fakultät der Universität Hamburg.

vorgelegt von:

Ruimeng Zhuang

aus Jiangsu, China

Hamburg 2023

Angenommen von der 19.09.2023

Medizinischen Fakultät der Universität Hamburg am:

Veröffentlicht mit Genehmigung der

Medizinischen Fakultät der Universität Hamburg.

Prüfungsausschuss, der/die Vorsitzende: Prof. Dr. Walter Fiedler

Prüfungsausschuss, zweite/r Gutachter/in: Prof. Dr. Manfred Jücker

Index

1 Introduction

1.1 Leukemia

Leukemia was the fifteenth most often diagnosed cancer worldwide in 2020, with 474,591 cases and 311,594 deaths, making it the tenth leading cause of death due to malignant illnesses (Sung et al., 2021). Multiple courses of induction chemotherapy, and allogenic hematopoietic stem cell transplantation or palliative care are the main treatment concepts for acute leukemia (Roboz, 2011).

1.1.1 Acute Myeloid Leukemia (AML)

AML is a heterogeneous disease characterized by a block in differentiation and uncontrolled proliferation of immature myeloid leukemia cells that affect hematopoietic stem and progenitor cells (Koenig et al., 2020; Swaminathan and Wang, 2020). It accounts for 15 to 20 percent of acute leukemia cases in children and 80 percent in adults (Lagunas-Rangel et al., 2017). To date, AML remains the most common acute leukemia in adult patients ("Acute Myeloid Leukemia Treatment (PDQ®)–Patient Version - National Cancer Institute," 2022). Chromosomal translocations occurs in 30- 40% of AML patients, whereas the remaining 60-70 percent have a normal karyotype. Currently, according to World Health Organization (WHO) and International Cancer Conference (ICC) in 2022, diverse recurrent molecular aberrations with prognostic and predictive impact are
1.1.1.1
known.

FMS-like tyrosine kinase 3 (FLT3)

The most prevalent genetic changes in AML are mutations in FLT3, which are found in around one-third of newly diagnosed adult patients (Papaemmanuil et al., 2016). FLT3 is a transmembrane ligand-activated receptor tyrosine kinase that is generally expressed by hematopoietic stem or progenitor cells and is involved in

the development of both the myeloid and lymphoid lineages (Grafone et al., 2012). The wild-type FLT3 (FLT3-WT) protein stays monomeric and inactive (Griffith et al., 2004). FLT3 receptors dimerize after attachment of the FLT3 ligand (Gilliland and Griffin, 2002) resulting in conformational FLT3 activation which promotes cell survival, proliferation, and differentiation via a variety of signaling pathways including PI3K, RAS and STAT5 (Grafone et al., 2012). In 25% of AML patients an Internal tandem duplications (FLT3-ITD) is observed. 75-80 percent of the Flt3-ITD involve exon 14 locate inside the juxtamembrane domain (JM domain). In 5% of AML patients a mutation in the second tyrosine kinase domain (FLT3-TKD) is observed which is in around 25% affecting codons 835 or 836 in exon 20. Flt3-ITD and Flt3-TKD are the most common forms of FLT mutations in AML (Gilliland and Griffin, 2002; Patnaik, 2018) and both are constitutively active, resulting in FLT3 signaling and cellular growth (Gilliland and Griffin, 2002). Ligand interaction at the plasma membrane (PM) causes the receptor JM domain to undergo a conformational shift and tyrosine phosphorylation, releasing an inhibitory contact. FLT3 kinase and downstream PI3K/AKT and RAS/extracellular signal–regulated kinase (ERK) pathways are activated as a result of this interaction. (Lv et al., 2021). Unlike FLT3-WT, the oncogenic mutant FLT3-ITD localizes to the endoplasmic reticulum and constitutively activates STAT signaling molecules (Hayakawa et al., 2000). However, the mechanism behind the altered localization and activation of downstream signaling pathways has long been a source of discussion in research.

Until recently, a group from the Children's Hospital of Philadelphia and the University of Pennsylvania Perelman School of Medicine identified potential palmitoylation sites on the FLT3 protein through comparative and bioinformatic analysis of the FLT3 amino acid sequence. Biochemical experiments show that both endogenously and exogenously expressed FLT3-WT, FLT3-ITD and the active mutants FLT3-D835Y of kinase structural domains all undergo an equal

degree of palmitoylation modification occurring at the cysteine at position 563 (C563). Interestingly, mutation at this site leads to relocalization of FLT3-ITD (FLT3-ITD/C563S) to the cell membrane and reactivation of PI3K/AKT and RAS/ERK signaling pathways, while maintaining activation of STAT5 (Lv et al., 2021). However, mutation at this locus does not affect at all the localization of FLT3-WT and FLT3-D835Y mutants and their activation of downstream signaling pathways. These evidences suggest that palmitoylation specifically affect the biological function of the oncogenic mutant FLT3-ITD.

Because the genetic basis of AML in individuals with a normal karyotype is still unknown, researchers have focused on finding particular gene alterations (Naseem et al., 2021). Changes in one gene alone are not enough to cause leukemia. Instead, multifunctional changes representing early and late events have been currently accepted as the model of leukemogenesis (Tebbi, 2021). As it was recognized as traditional treatment, the nucleoside analog cytarabine, given in conjunction with an anthracycline as induction therapy, has been used as the most effective treatment, followed by multiple cycles of high-dose cytarabine and/or an allogenic stem cell transplant (SCT) in patients who achieve complete remission (CR) (Fröhling et al., 2006). However, thanks to next-generation gene sequencing technology, the detection of mutations in AML offers patients the possibility of access to precision medicine and personalized treatment (Cai and Levine, 2019). Besides, benefited from the performance of a growing number of laboratory investigations and clinical trials, now we have a better understanding of how AML develops from a molecular perspective, which has allowed us to update the classification of the disease. Additionally, genomic diagnostics and the evaluation of measurable residual disease have advanced significantly, and new therapeutic agents like FLT3, IDH1, IDH2, and BCL2 inhibitors have been developed successfully (Döhner et al., 2022).

Core binding factor-AML (CBF-AML) and c-Kit mutation

Core binding factor-AML (CBF-AML) is formed by the mutations t(8;21)(q22;q22) and inv(16)(p13;q22). Adults with CBF leukemia have 12.8–46.1% activation of the c-klt[1][2] mutation, among which, 20–25% of the instances are t(8;21), while 30% of the cases are inv(16) (Ayatollahi et al., 2017). Despite being thought to have a better prognosis than other leukemia subtypes, CBF-AMLs are a diverse collection of diseases, and contemporary treatment frequently results in relapses and the accompanying morbidity and death (Sinha et al., 2015). Additionally, a clinical investigation has demonstrated that the c-KIT mutation is a poor risk factor for pediatric CBF-AML (Shafik et al., 2022).

c-Kit was initially called stem cell factor receptor because of its function in hematopoietic stem cell survival, self-renewal, and differentiation. As a member of the RTKs type III family, c-Kit is structurally identical to flt3 and it is closely related to AML. Most human AML cells express wild-type c-Kit, which is frequently constitutively phosphorylated (Masson and Rönnstrand, 2009). The amount of N-linked glycosylation determines the size of human c-Kit, which comes in two sizes: 140kD and 155kD (Arakawa et al., 1991; Majumder et al., 1988). The findings of a study indicate that c-kit mutations adversely affect the relapse and increase in white blood cells in people with CBF-AML. However, these alterations don't significantly affect a patient's prognosis (Ayatollahi et al., 2017). The Ras-Raf-MAP kinase cascade, Src family members, JAK/STAT pathway, and phosphatidylinositol 3-kinase (PI3K) are among the main signal transduction elements that are involved in the c-Kit downstream signaling pathways (Linnekin, 1999). The PI3K pathway can be activated by c-Kit once it binds to SCF in direct or indirect ways. Direct activation function through the binding to Tyr721 in c-Kit whereas binding to GAB2 followed by activation of Src-mediated phosphorylation results by indirect activation. The PI3K-mediated increase of phosphatidylinositol 3,4,5-trisphoshate directly recruits and stimulates the

downstream signaling molecule AKT which enhances cell survival in several ways. However, based on the fact that GAB2 expression levels change between different types of cells and it interacts with various c-Kit isoforms differently, the manner of indirect activation is more complicated than direct activation (Liu, 2006). Another signaling pathway stimulated by c-Kit is the mitogen-activated protein kinase (MAPK) pathway (Wandzioch et al., 2004). The activation of downstream pathway is mediated by Tyr703 and Tyr936 of c-Kit (Smalley et al., 2009) which further combines with Grb2 to form a complex after interacting with Sos (Pathania and Rawal, 2020). It is evident that Grb2 is involved in the activation of PI3K pathway and MAPK pathway at the same time, revealing the crosstalk mechanism between different downstream signaling pathways of c-Kit. Src family kinases (SFKs) are another important effector located at the signaling pathway which is downstream of c-Kit (Lennartsson et al., 1999). SFKs are also effectors that function as a crossroads in different downstream signaling pathways of c-kit (Pathania et al., 2021). Studies have demonstrated that blocking ligand-induced c-Kit can be accomplished by inhibiting SFK family kinases using inhibitors. According to the aforementioned experimental findings, Lyn could be crucial to the internalization of c-Kit (Broudy et al., 1999).

1.2   Metabolic reprogramming in hematological malignancies

1.2.1 Warburg Effect

Warburg discovered in the 1950s that tumor cells have a different metabolic pattern than normal cells, and that the glycolytic pathway of tumor cells remains active even when there is enough oxygen, a metabolic shift known as aerobic glycolysis or the Warburg effect, one of the most common and well-known metabolic reprogramming in tumor cells. Recently, the renewed interest in the Warburg effect has enlightened researchers that

there could be an opportunity to explore the mechanisms of tumorigenesis in terms of metabolic abnormalities (Pascale et al., 2020).

1.2.2 Fatty Acid Synthase (FASN) and hematological malignancies

Although some progress has been made in the study of metabolic abnormalities like glucose metabolism in AML cells (Chen et al., 2014; Forte et al., 2020; Gu et al., 2021; Jones et al., 2018; Raffel et al., 2017), the role of abnormal lipid metabolism in AML cells has not been fully studied. However, breakthroughs in lipid metabolism analysis in other hematological malignancies may provide new therapeutic options for AML. It has been shown that lipid pathway synthesis is abnormally active in haematological tumours (Stuani et al., 2018). FASN is a crucial enzyme in the last phase of fatty acid biosynthesis that has been intensively studied in solid tumors such as breast, bladder, and prostate malignancies in recent years (Menendez and Lupu, 2017, 2007; Pandey et al., 2012). In the meanwhile, antitumor efficacy has been observed for certain FASN-specific inhibitors, including C75, canthaxanthin and orlistat (Merino Salvador et al., 2017). In ALL, the expression of FASN at the mRNA level was found to be considerably greater in relapsed ALL patients than in freshly diagnosed patients (Ghaeidamini Harouni et al., 2020). Besides, FASN expression was also shown to be high in primary exudative lymphoma (PEL), mantle cell lymphoma (MCL) and multiple myeloma (MM) (Bhatt et al., 2012; Gelebart et al., 2012; Wang et al., 2008). In a trial of US patients with diffuse large B-cell lymphoma (DLBCL), high expression of FASN was observed to correlate with poor prognosis and FASN was therefore used as an independent prognostic indicator to assess DLBCL patients after chemotherapy (Danilova et al., 2013).

1.2.3 FASN inhibitors

Since late 20th century, FASN inhibitors have been produced and certain FASN-specific inhibitors, including C75, canthaxanthin and orlistat have shown antitumour efficacy (Merino Salvador et al., 2017). However, first-generation

inhibitors, such as cerulenin, have caused unwarranted adverse effects (Röhrig and Schulze, 2016). Therefore, successive developments of second-generation FASN inhibitors have been made since then (Oh et al., 2020). TVB-3166, as a reversible and selective imidazopyridine-based FASN inhibitor (Oh et al., 2020), along with TVB-2640, TVB-3664, TVB-3693, and TVB-3567, are developed by 3-V-Biosciences and have demonstrated antitumor activity *in vitro* and *in vivo*. It has been shown to be effective in a number of preclinical studies for the treatment of several solid tumours, including but not limited to breast, prostate, colorectal and lung cancers (Benjamin et al., 2015; Heuer et al., 2017; Jafari et al., 2019; Long et al., 2017; Tao et al., 2019; Ventura et al., 2015; Zaytseva et al., 2018).

1.2.4 FASN related signaling pathways

1.2.4.1 PI3K–AKT–mTOR

Activation of the PI3K–AKT–mTOR pathway is one of the most common abnormalities in human malignancies and it can be caused by a variety of genetic mutations (Vivanco and Sawyers, 2002). Many biological functions are controlled by the PI3K–AKT–mTOR pathway, including glucose absorption and metabolism, protein synthesis, cell growth, and cell survival (Hollander et al., 2011). The mechanism of FASN activation in response to cell metabolism and growth signals has been demonstrated to be driven by SREBP-1, ZBTB7A and p53 family transcription factors which activate FASN gene expression downstream of the PI3K–AKT–mTOR signaling cascade (Choi et al., 2008; Van de Sande et al., 2005). Conversely, the reversal effects from FASN to PI3K–AKT–mTOR has not yet been clearly clarified so far in human AML cell lines. Therefore, there is still a large research gap in investigating the functional role of FASN in human leukemia cell lines.

1.2.4.2 Ras/RAF/MEK/ERK signaling pathway

The Ras/RAF/MEK/ERK (MAPK, mitogen-activated protein kinase) signaling pathway was first discovered in the 1970s and 1980s as Ras was demonstrated to be a small GTPase and subsequently N-terminal truncated form of the RAF Ser/Thr kinase (RAF1 or CRAF) was found by means of deep investigations of viral oncogenes (Bonner et al., 1984, 1985; Jansen et al., 1984, 1983; Kozak et al., 1984; Rapp and Todaro, 1978).

However, the other two components of this signaling pathway MEK (mitogen-activated protein kinase kinase) and ERK (mitogen-activated protein kinase) were not identified as cytoplasmic protein kinases activated by mitogens until the 1990s (Ahn et al., 1990; Bonner et al., 1985; Boulton et al., 1991; Crews and Erikson, 1992; Ray and Sturgill, 1988). On this basis, RAF was identified as the upstream kinase of MEK and the first direct actor of Ras in the following two years (Crews and Erikson, 1992; Rapp et al., 1983), thus revealing the complete picture of the MAPK signalling pathway and setting a milestone for cellular perception of external stimuli. Similar to PI3K-AKT-mTOR, FASN activity has also been reported to be closely correlated with the MAPK signalling pathway (Ventura et al., 2015). For example, The ERK1/2 kinase cascade has been reported to be involved in cellular fatty acid absorption in skeletal muscle based on the action of the ERK1/2 inhibitor PD98059 (Turcotte et al., 2005). Intriguingly, few papers have reported regulatory patterns between the MAPK pathway and FASN in hematological malignancies.

1.2.4.3 Hedgehog (Hh) / Gli1 signaling pathway

The molecular mechanism by which the canonical Hh signaling pathway activates Gli1 is through inactivation of the Hh ligand by binding to protein patched homolog 1 (PTCH1), which then mediates the G-coupled receptor-like signal transducer Smoothened homolog (Smo) release and blockade of its inhibitory partner, the

suppressor of fused homolog (SuFu). In contrast, activation of Gli1 protein mediated by signaling molecules in pathways such as mTOR/S6K1 and mitogen-activated protein kinase/extracellular signal-regulated kinase is referred to as non-classical Hh signaling (Teperino et al., 2014; Wang et al., 2012). It has been reported that FASN blockade via siRNA reduced Gli1 levels in gastric cancer cells, suggesting that FASN may play a role in gastric cancer tumorigenesis and metastasis as a regulator of the Hh signaling pathway effector Gli1(Sun et al., 2018). However, as with the regulatory relationship between FASN and mTOR, there is still a long way to go in terms of signaling pathways between FASN and Gli1 in haematological malignancies, although some of this research has progressed in other tumors.

1.2.4.4 RPS6 (Ribosomal Protein S6) as an interaction point between pathways (cross-talk)

RPS6 is the downstream effector of the PI3K/AKT/mTORC1 and MAPK pathways, and it serves as a convergence node of these two signaling pathways (Yi et al., 2021). It has been reported that these two signaling pathways can function synergistically on regulation of RPS6 phosphorylation (Carrière et al., 2008; Lai et al., 2015; Ma et al., 2005; Mukhopadhyay et al., 1992). However, the precise functions of RPS6 phosphorylation remain unknown (Yi et al., 2021). The 40S ribosomal protein S6 is multiply phosphorylated as a result of cell growth activation. The kinase RPS6KB1 also called p70S6K is known for regulating this event. Both isoforms of the kinase, the p70S6K in the cytoplasm and the p85S6K in the nucleus, are produced from a single gene that is triggered by a complicated series of phosphorylation events (Ferrari and Thomas, 1994). p70S6K is well known for its function in controlling cell size, cell survival, and cell cycle progression. Activation of p70S6K up-regulates ribosomal biosynthesis and increases the cell's ability for translation in response to mitogen stimulation (An et al., 2003)

2 Material and Methods

2.1 Material

2.1.1 Device

Autoclave: Evo 120, MediTech (Wedemark, Germany)

Blot chamber and Trans-Blot Electrophoretic Transfer Cell, Bio-Rad (Munich, Germany)

Centrifuges 5415 C 5415 D, 5415 R, Eppendorf (Hamburg, Germany)

Counting chamber Neubauer, Braun (Melsungen, Germany)

Glassware Schott (Mainz, Germany)

Heating block Eppendorf Thermomixer 5426, Eppendorf (Hamburg, Germany)

Horizontal shaking device: Rocky N, Fröbel Labortechnik (Lindau, Germany)

Incubator: Heraeus (Hanau, Germany)

Light microscope: Labovert, Leitz (Stuttgart, Germany)

Live cell imaging system Incucyte® Zoom S3 live cell imaging system, Sartorius, Essen BioScience (Ann Arbor, Michigan, USA)

Luminescent Image Analyzer: LAS-4000, Fujifilm (Düsseldorf, Germany)

Magnetic stirrer Ikamag RH, IKA laboratory equipment (Staufen, Germany)

NanoDrop 2000c Thermo Fisher Scientific (Waltham, MA, USA)

pH electrode SenTix 21 (WTW, Weilheim, Germany)

pH meter: CG 820, Schott-Devices (Ludwigshafen, Germany)

Pipettes: 0,1-10, 10-100, 20-200, 100-1000µl, Eppendorf

Pipetting aid: Accu-jet pro, Brand (Wertheim, Germany)

Plate reader: Infinite M200, Tecan (Männerdorf, Germany)

Power supplies: PowerPac universal, PowerPac 200, Bio Rad

(Munich, Germany)

Precision scale: UniBloc, Shimadzu (Duisburg, Germany)

Research (Hamburg, Germany)

Safety cabinet class ll: HERA safe Type HS12, Heraeus (Hanau, Germany)

Scale: Type PM 2000, Mettler (Gießen, Germany)

Scientific Co. Inc (Edison, New Jersey, USA)

SE600 Cooled Vertical Electrophoresis Unit,

    18x16cm2, Hoefer (Boston, MA, USA); Biorad Chamber

Shaking device for bacteria: Model G25 Incubator Shaker, New Brunswick

Ultrapure water system Synergy UV, Millipore (Schwallbach, Germany)

Varifuge 3.0R, Heraeus (Hanau, Germany)

Vortex device: MS2 Minishaker IKA-Werk (Staufen, Germany)

Water bath: Typ 1002, Typ 1012 GFL (Burgwedel, Germany)

2.1.2 Consumables

Cell culture bottles: T75 (75cm2), T175 (175cm2), greiner bio-one;

Sarstedt (Nümbrecht, Germany)

Cell culture plates:

6-well, Greiner bio-one, Sarstedt (Nümbrecht, Germany)

96-well, flat, Greiner bio-one, Sarstedt (Nümbrecht, Germany)

TC dish, 100mm, standard, Sarstedt (Nümbrecht, Germany)

Cover slips: Laboratory Glassware, Superior-Marienfeld (Lauda-Königshofen, Germany)

Cryo tubes Nunc A/S Thermo Fischer Scientific (Waltham, MA, USA)

Disposable pipettes: 5, 10 and 25ml, Sarstedt (Nürnbrecht, Germany)

Filters: Acrodisc 25mm Syringe Filter w/0.45µm HT Tufffryn

Membrane, Pall Corporation (New York, USA)

Nitrocellulose membrane: Amersham Protran 0.45µm NC; Amersham / GE

Healthcare (Amersham, England)

Pipette tips: 10, 200, 1000µl Eppendorf (Hamburg, Germany)

Reaction tubes: 1.5 and 2.0ml Eppendorf (Hamburg, Germany)

Syringes: Injekt 10ml, Braun (Melsungen, Germany)

Tubes: 15 and 50ml, Sarstedt (Nümbrecht, Germany)

Whatmanpaper: Whatman 6.5cmx14.5cm; GE Healthcare

(Amersham, England)

2.1.3 Buffers and solutions

Antibody Diluent

    144mM NaCl

    10mM Tris-HCl pH 8.0

    0.5% Tween

Blocking solution:

    144mM NaCl

    10mM Tris-HCl pH 8.0

    0.5% Tween

    50g/l milk powder

    2.5% milk powder

Concentration gel:

    380mM Tris-HCl pH 6.7

    4.02% Acrylamid

    0.1% SDS

    0.08% TEMED

    0.15% APS

LB-Broth agar plates:

    250ml LB-Broth medium (Difco)

    LB-Broth, Miller (Luria-Bertani), Becton, Dickinson and Company (Le Pont deCaix, France)

    3.75g Agar

    dimethylsulfoxide (DMSO) Fluka (Buchs, Switzerland)

LB-Broth Medium:

    6.25g LB-Broth medium (Difco)

    LB-Broth, Miller (Luria-Bertani), Becton, Dickinson and Company (Le Pont deCaix, France)

250ml ddH2O

NP40 lysis buffer:

50mM Hepes

150mM NaCl

1% NP40

2% Aprotinin

2mM EDTA

50mM NaF

10mM NaPPi

10% Glycin

1mM Sodium orthovanadate

1mM Phenylmethylsulfonyl fluoride (PMSF)

Seperation gel:

375 mM Tris-HCl pH 8.8

10% Acrylamid

0.1% SDS

0.07% TEMED

0.07% APS

1xPBS pH 7,4:

8mg/ml NaCl

0.2mg/ml KCl

1.78mg/ml Na2HPO4x2H2O

0.24mg/ml KH2PO4x2H2O

pH was adjusted with NaOH

10x running buffer:

144g/l glycine

30g/l Tris/Base

1x running buffer for SDS page 10%:

10x running buffer

0.1% SDS

89.9% ddH2O

Cathode buffer

99.875% 1x running buffer

0.125% Dithiothreitol

10x TBS:

84,15g/l NaCl

10% 1M Tris HCl pH 8,0

TBS-0,5% Tween

5,5g/l Tween 20

10% 10x TBS

Transfer buffer:

192mM Glycin

25mM Tris

20% Methanol

0.1% SDS

FCS GIBCO, Thermofisher Scientific (Waltham, MA, USA)

medium for HEK-293T DMEM: 10% FCS, 1% P/S

medium for Kasumi1 cell line: RPMI, 20% FCS, 1% P/S

RPMI GIBCO, Thermofisher Scientific (Waltham, MA, USA)

OptiMEM GIBCO, Thermofisher Scientific (Waltham, MA, USA)

Penicilline/Streptomycine GIBCO, Thermofisher Scientific (Waltham, MA, USA)

Puromycin Sigma-Aldrich (Taufkirchen, Germany)

protein marker SpektraTM Multicolor Broad Range Protein Ladder

(SM1841)

Trypan blue solution sigma-aldrich (Taufkirchen, Germany)

2.1.4 Kits

Chemiluminescence substrate (Super Signal West Dura) Thermo Fisher Scientific

(Waltham, Massachusetts)

DC-Protein Assay Bio-Rad (Munich, Germany)

NucleoBond Xtra Midi Macherey-Nagel (Düren, Germany)

P3000 Gibco Thermo Fisher Scientific (Waltham, MA, USA)

transfection reagents Lipofectamine, Gibco Thermo Fisher Scientific
(Waltham, MA, USA)

2.1.5 Antibodies

Primary antibodies

panAKT #4685S rabbit monoclonal antibody Cell Signaling
Technology (Beverly, MA, USA)

pAKT S473 #4060S rabbit monoclonal antibody Cell Signaling
Technology (Beverly, MA, USA)

FASN #48357 rabbit monoclonal antibody Santa Cruz
biotechnology (Heidelberg, Germany)

Phospho-LYN #70926 rabbit monoclonal antibody Cell Signaling
Technology (Beverly, MA, USA)

MAPK #4695S rabbit monoclonal antibody Cell Signaling
Technology (Beverly, MA, USA)

pMAPK #4377S rabbit monoclonal antibody Cell Signaling
Technology (Beverly, MA, USA)

S6 #2217S rabbit monoclonal antibody Cell Signaling
Technology (Beverly, MA, USA)

pS6 #2215S rabbit monoclonal antibody Cell Signaling
Technology (Beverly, MA, USA)

Secondary antibodies

anti-mouse IgG HRP-linked antibody, #7076, Cell
Signaling Technology (Beverly, MA, USA)

anti-rabbit IgG HRP-linked antibody, #7074, Cell
Signaling Technology (Beverly, MA, USA)

2.1.6 Bacterial strain

Xl1Blue Pierce Thermo Fisher Scientific (Waltham, MA, USA)

2.1.7 Vectors

PLKO.1-puro vector encoding FASN, PLKO.1 non-target (scrambled, SCR) shRNA were purchased from Sigma-Aldrich (Taufkirchen, Germany).

2.1.8 Inhibitors

TVB3166 was given kindly from Maxim Kebenko

2.1.9 Software

Microsoft Office 2007

Graphpad Prism: Version 8.2

AIDA Image Analyzer: Version 3.44

Zotero: 6.0.20

2.2 Methods

2.2.1 Culturing of cells

By operating in a safety cabinet class ll, cells were shielded from contamination. Autoclaving was used on equipment that came into touch with cells. Equipment utilized beneath the safety cabinet was cleaned with an ethanol solution diluted to 70%. Trypsin (when used for HEK293 cell culture) was warmed to room temperature before use, and medium was warmed in a 37°C water bath. PBS was stored at ambient temperatures. Cells were grown in an incubator with 5% CO_2 at 37°C.

Thawing of cells

Cells were kept at -80°C in cryo tubes filled with 90% FCS and 10% DMSO. They were promptly moved to a warm medium after being briefly reheated in the water bath for defrosting. The media was withdrawn using the pipetting controller after the cells were centrifuged for 5 minutes at room temperature and 1400 rpm to remove the DMSO. The cell pallet was then transferred to a T75 cell culture bottle and resuspended in 10ml of warm media.

2.2.2 Passaging of cells

The replacement of the medium or addition of fresh media was used to sustain cultures. Alternatively, centrifugation with subsequent resuspension at 5×10^5 viable cells/mL was used to create cultures. A cell density of 5×10^5 to 2×10^6 viable cells/mL was maintained. Every two to three days, depending on the cell density, new media was added.

2.2.3 Freezing of cells

When the density of the cells reached around 1×10^6 viable cells/mL, the cells were frozen. The cells were centrifuged for five minutes at 14000 rpm and room temperature. The pallet was then immediately transferred to a cryo tube after being resuspended in 90% FCS and 10% DMSO. The cryo tube was kept in a freezing device for 24 hours before being transferred to the -80°C nitrogen tank.

2.2.4 Counting of cells

A Neubauer cell counting chamber was used to assess cell concentrations. A mixture of 10µl of trypan blue solution and 10µl of cell suspension was aliquoted and pipetted between the cover slip and the chamber. Under a microscope, the chamber's cells were counted. For each cell line, this was done three times. The average was divided by the second dilution factor. The quantity is equivalent to 10^4 cells in a milliliter.

2.2.5 Incucyte Zoom

2.2.5.1 Proliferation

Kasumi1 cells were plated into a 96-well plate with 10,000 cells per well for the inhibitor treatment, and each well received 100µl of RPMI 20% FCS 1% P/S for incubation. Using the IncuCyte Zoom imaging equipment from Essen Bioscience, cell confluence was calculated. 100µl of the inhibitor solution was added after 24 hours. Additionally, 10000 Kasumi1 SCR and FASN knockdown cells were plated into a 96-well plate from Greiner Bio One, Frickenhausen, Germany, and cultured in 200µl of RPMI 20% FCS 1% P/S and 1.5 g/ml puromycin.

2.2.6 Lentiviral knockdown of FASN

2.2.6.1 Transformation

100ng of plasmid DNA was introduced after defrosting 100 of XL1 blue bacteria on ice. After gently blending, the solution was incubated for 30 minutes on ice. The bacteria suspension was then shock heated to 42°C for one minute and put back on ice right away. The mixture was then added, and it was then incubated at 37°C for an hour. Then, 150µl of the suspension was pipetted onto 100 g/ml LB Agar plates. Ampicillin for picking, then uniformly distribute using a spreader rod. The plates were dried and then incubated at 37°C overnight upside down. The next day, colonies were selected and added to the LB broth medium using a sterile 10µl pipette tip.

2.2.6.2 Plasmid prep

The bacteria suspension was put into centrifuge tubes, which were then centrifuged in the GSA rotor for 10 minutes at 4°C and 5000rpm. After being inverted five times, the pallet is resuspended in 8ml of resuspension buffer (RES) and then incubated in 8ml of lysin buffer (LYS) for five minutes. The solution was then inverted and the neutralizing buffer (NEU) was added until the blue hue vanished. The suspension was filtered through the columns (NucleoBond Xtra Columns) after they had each been attached to a filter holder and filled with 12ml of equilibration buffer (EQU). 5ml EQU was used to wash the columns and filters, and then the filters were discarded. Washing buffer (15 ml) was poured into the filter holder. Each 50 ml tube containing the eluate was then filled with 5 ml of elution buffer (ELU). Each eluate was then divided into 830µl aliquots and put into 6 1.5 ml tubes with 580µl of isopropanol in each. The tubes were turned over and centrifuged for five minutes at 13200 rpm at room temperature. The supernatant was then discarded, 200µl of 70% ethanol (which was not included in the NucleoBond Xtra plasmid purification Kit) were added, and the mixture was centrifuged once more at 13200 rpm for 5 minutes at room temperature. The DNA was dried after as much supernatant as

feasible was removed. Each tube was then filled with 20μl of sterile, distilled water, and kept at room temperature for 5 minutes. The tubes were then gently swirled, the 6 tubes were combined in one tube with 80μl of sterile water, and the tube was gently whirled once again. The plasmid solution was frozen at -20°C while the DNA concentration was measured in the NanoDrop 2000c (Thermo Scientific).

2.2.6.3 Transfection of HEK293T

HEK293T had been plated 4 days prior in a single 10 cm dish per knock down with $2x10^5$ cells per dish. The day of the transfection, 8g VSVG and gagPol and 20μl of P3000 reagent were added to 2.5g of each vector's DNA for dilution. One tube containing 720μl of OptiMEM and 30μl of Lipofectamine was produced and whisked for each knockdown. Quickly, all of the solutions were revealed. One of the DNA solutions was added to each OptiMEM and lipofectamine solution after which it was inverted three times and let to sit for 10 minutes at room temperature. In the interim, 5ml of DMEM 10% FCS without Penicillin/Streptomycin was substituted for the HEK293T's original medium in the 10cm plates. The HEK cells were then treated with the DNA solutions and incubated for three hours. In the meanwhile, 2ml of media containing $5x10^5$ Kasumi1 cells was used to plate the cells onto 6 well plates. Each knockdown and cell line required at least one plate. The HEK cells are then given 2.5ml of DMEM 10% FCS with Penicillin/Streptomycin after three hours of incubation.

2.2.6.4 Transduction

A 10ml syringe was used to extract the medium from HEK293T 24 hours after transfection. The viral supernatant was then put into a 15ml tube after a 22μl filter was attached to the syringe. The target cells' media was then taken out, while substituted by new culturing medium and 2ml of viral supernatant. Each plasmid was transduced into a separate well. At -80°C, the remaining viral supernatant was

frozen. After 48 hours, the process was done again. The virus-containing media was taken out of the target cells 24 hours later. 4ml of RPMI with 20% FCS 1% P/S with 1.5g/ml Puromycin was administered to the cells in order to select them. The control wells also received 4ml of 1.5g/ml Puromycin-containing RPMI 20% FCS 1% P/S. When every cell in the control wells had died, the selection process was deemed to be complete.The target cells were liberated from their media.

2.2.7 Western Blot

2.2.7.1 Production of whole cell lysates using NP40 lysis buffer

Just before using the NP40 lysis solution, the substances Aprotinin, Sodium orthovanadate, and Phenylmethylsulfonyl fluoride (PMSF) were added and maintained on ice. Two days earlier, 1×10^6 cells from the cells had been seeded onto 10cm plates. Cell pellets were created by centrifuging the cells. Then, each cell pellet received 1ml of NP40 lysis solution, which was then incubated for three minutes on ice. Prior to being transferred to a 1.5ml reaction tube, the solution was pipetted up and down 10 times. The reaction tube was then centrifuged for 10 minutes at 12000rpm and 4°C. The supernatant was centrifuged, transferred to a new 1.5ml reaction tube, and then frozen at -80 °C until needed. The pallet was thrown away.

2.2.7.2 Determination of the protein concentration using the DC protein assay kit

The DC protein assay kit is used to measure the protein content in protein lysates. Proteins react with copper in an alkaline environment, which reduces the Folin reagent and produces a blue hue. The protein lysates were defrosted on ice before being administered in triplicates of 5µl to a micro plate. Bovine serum albumin was prepared in concentrations of 0.125 mg/ml, 0.25 mg/ml, 0.5 mg/ml, 0.75 mg/ml, 1 mg/ml, 1.25 mg/ml, and 1.5 mg/ml, and placed into a microplate with 5 l each as triplicates for a standard curve. Then, 25µl of a 2% reagent S in reagent A dilution

was applied to each well. The micro plate was filled with 200µl of reagent B and let to sit at room temperature for 15 minutes. The microplate was measured using an adsorption mode, a 750nm wavelength, a 9nm range, and 25 flashes in a microplate reader. The protein concentration was determined using a linear standard curve and the extinctions of the protein samples.

2.2.7.3 SDS-page and electrophoresis

Different proteins were separated according on size using SDS-page. 13ml of running gel was added to the gel tray after it had been assembled according to the manufacturer's instructions, and it was then covered with 600µl of isopropanol and left to sit at room temperature for an hour. After carefully draining the water from the isopropanol, 5ml of stacking gel was added, and 15 pocket comb were dropped into the gel to create 1.5 cm-long pockets. The stacking gel also underwent at least one hour of polymerisation. To produce identical protein concentrations, the protein lysates were defrosted on ice and diluted with NP40 lysis buffer. The lysates were then diluted 1.3:4 in a solution of 30% dithiothreitol (DTT), 70% loading buffer, and 70% loading buffer. The protein samples were quickly centrifuged at 13000 rpm after being heated at 95 °C for 5 minutes. The combs were taken off, water was used to eliminate air bubbles, and cathode buffer was added to the stacking gel's pockets before 40–60µl of the samples were applied to it. 3µl of protein marker were placed in one pocket of each gel. The blot chamber, which had been filled with running buffer, was then filled with the gel tray. Cathode buffer was placed in the top chamber. The loading buffer bands were then applied at voltages of no more than 120V until they reached the running gel and 175V until they reached the end of the gel.

2.2.7.4 Transfer and development

The gels were taken out of the gel trays and given a delicate ddH2O wash. Before use, nitrocellulose membrane pieces of 6.5cm by 14.5cm were humidified in ddH2O. The blot sandwich was assembled when the transfer trays were put into the transfer buffer. It was made up of two sponges, two pieces of Whatman paper measuring 6.5cm by 14.5cm, a gel and membrane in direct contact with one another, free of air bubbles. One transfer tray holds two sandwiches. The transfer chamber was then filled with transfer buffer until the blot sandwiches were completely covered, and the transfer trays were then put inside. The transfer chamber was subjected to a 65V voltage for two hours.

The membranes were rinsed in ddH2O for at least 2 minutes after the blot sandwiches were opened, the gels being discarded in the process. A pencil was used to make markers on the protein marker bands. The membranes were then stained with Penceau staining until protein bands were found, and depending on the proteins that were targeted, they were chopped down to useable sizes or divided into separate parts. The membranes were put in blocking solution and blocked at room temperature while gently shaking to eliminate Penceau staining. A washing solution containing the appropriate primary antibody in a dilution of 1:1000 was then added after the blocking solution had been in place for an hour. The membranes were then kept at 4°C overnight for incubation. The solutions were kept at 4°C until further use the following day after the antibody solutions had been withdrawn and sodium azide had been added at a concentration of 1:1000. Three times for a total of five minutes, the membranes were washed in TBS-0.5% Tween. The appropriate secondary antibodies were then diluted 1:5000 in washing solution and added, followed by an incubation period at room temperature. The membranes were then washed in TBS-0.5% Tween four times for a total of 15 minutes after the secondary antibodies had been removed after one hour. Thermo Fisher Scientific's LAS 4000 imager and Super Signal West Dura chemiluminescence substrate kit

were used to create the membranes.

2.2.8 Statistical Analysis

Unpaired t-Test was used to determine significance. The plots show significance as * for p0.05, ** for p0.005, and *** for p0.001. Error bars represent standard deviation.

To demonstrate the actual changes in phosphorylation, which are not caused by variations in total protein that can be created by protein production, the ratio between p-protein and total protein is determined.

The majority of the data analysis is based on the outcomes of total protein quantification using Ponceau red staining in order to more uniformly standardize the wb quantification section of the text.

3 Results

The major goal of this project was the analysis of the functional role of FASN for signal transduction in acute myeloid leukemia cells. Therefore, stable knockdowns of FASN were established in the AML cell line Kasumi. As shown in figure 1, expression of FASN was reduced by two independent lentiviral knockdown vectors by over 80%.
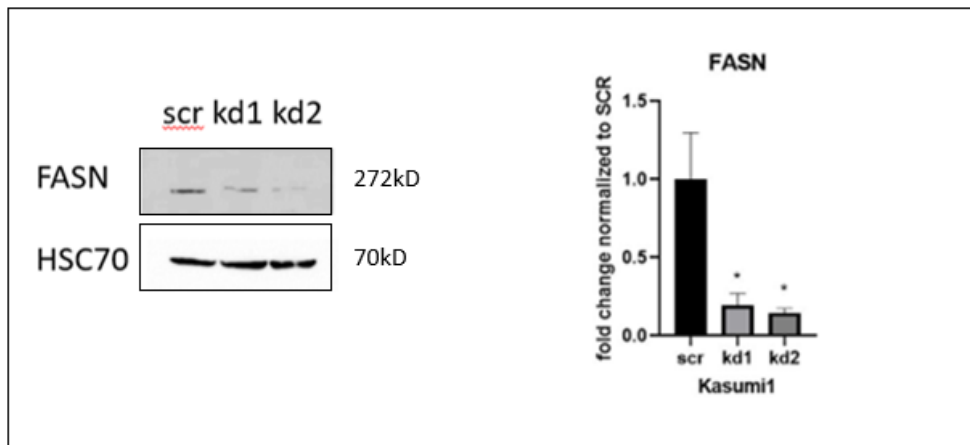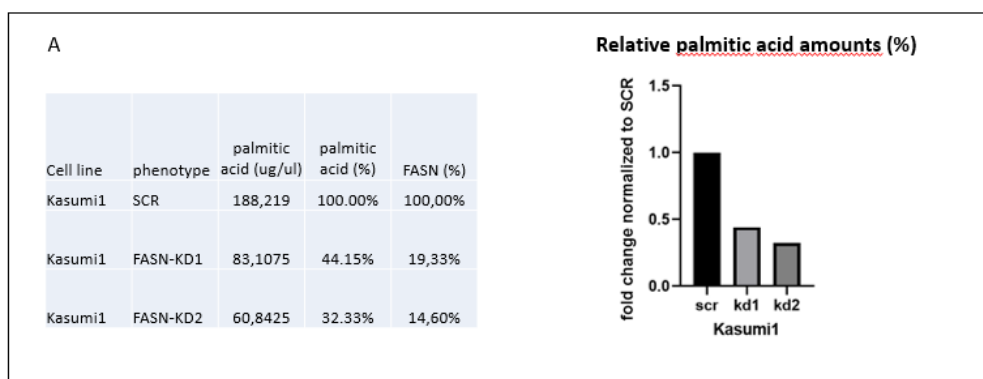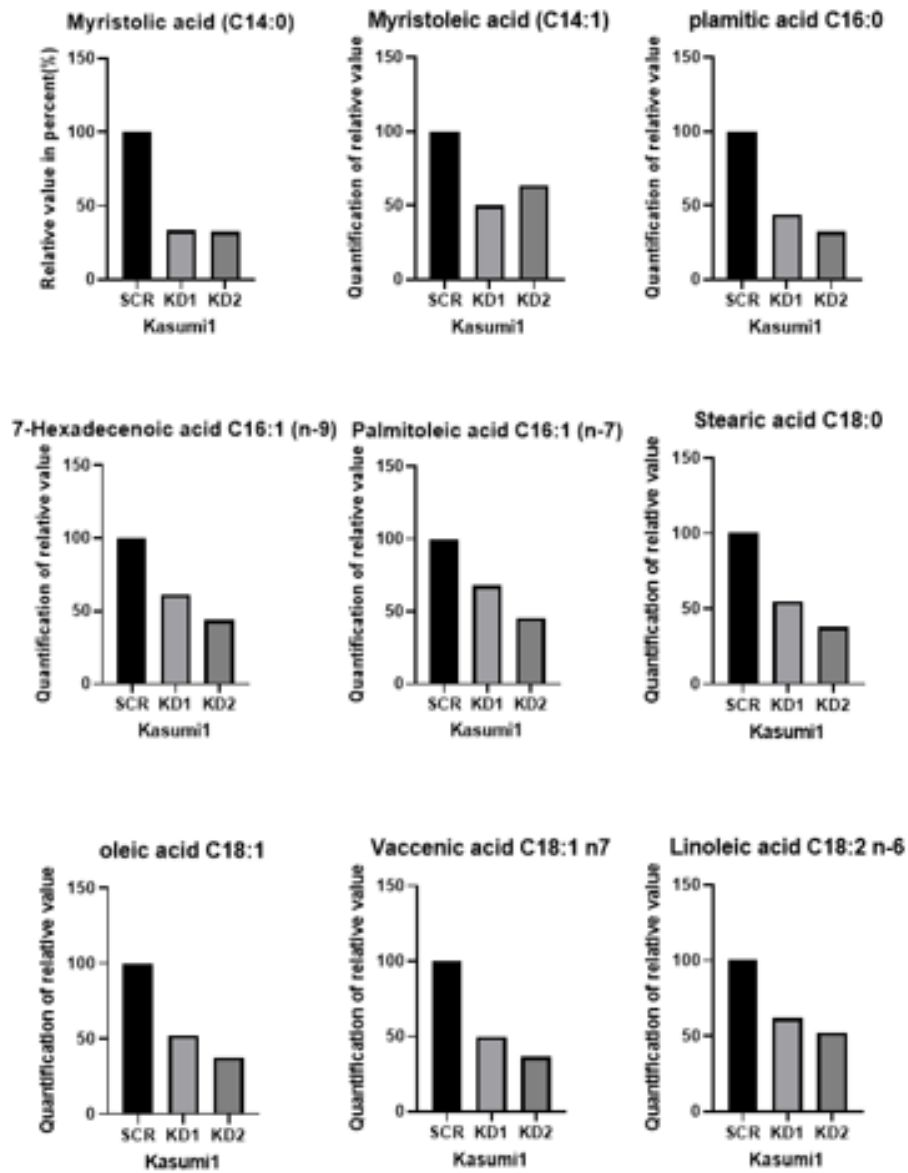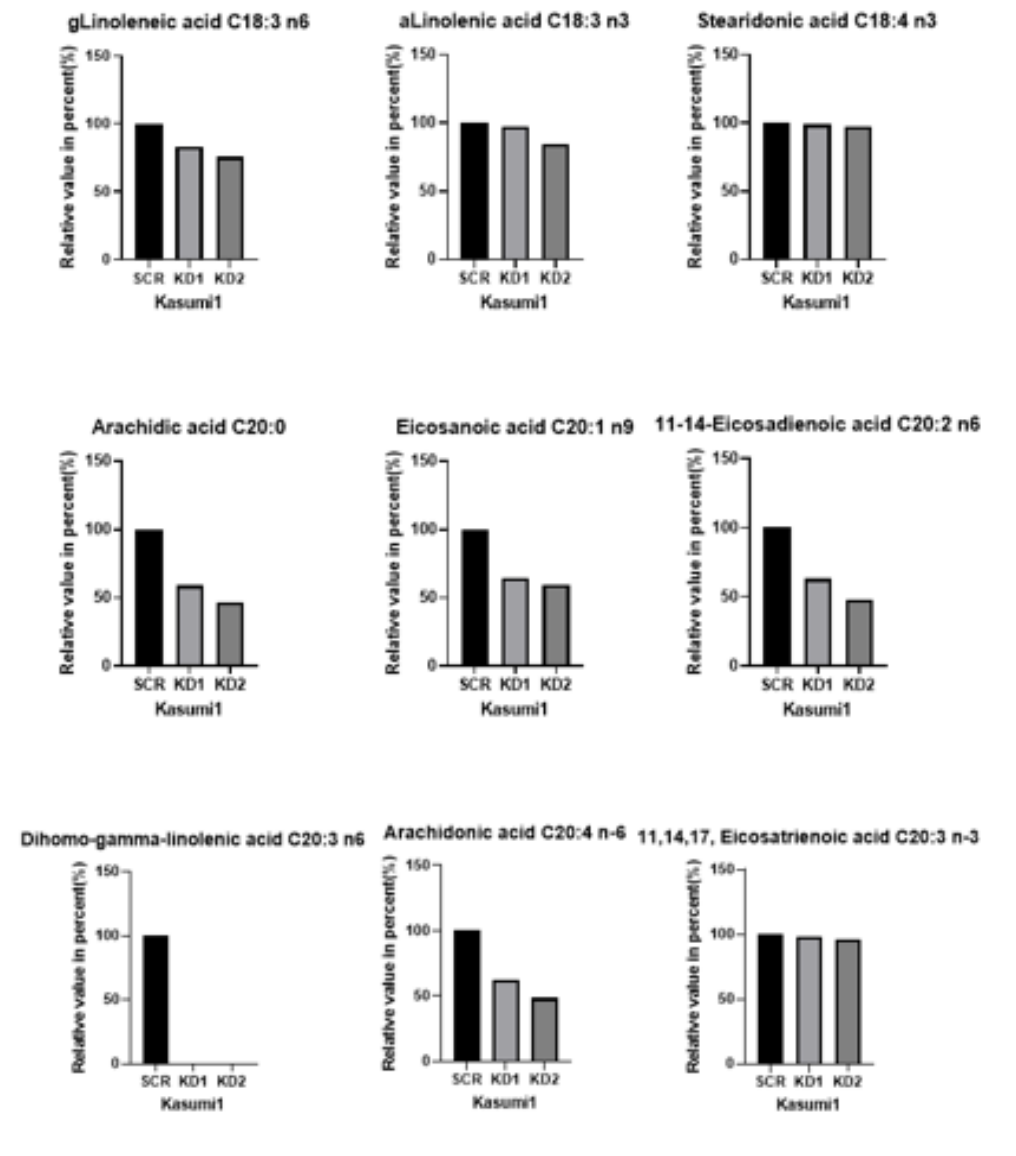

Figure 1. shRNA-mediated knockdown of endogenous FASN in Kasumi1 cells. FASN expression was detected in whole cell lysate by western blot. Kasumi1 FASN kd cell lines transduced with FASN shRNA (either with vector1 which is kd1 or with vector2 which is kd2) or Kasumi1 scr cell line transduced with non-targeting vector as a control for the baseline expression of FASN in Kasumi1 cell line. Western blot was performed in technical triplicates with whole cell lysates prepared by using NP40 lysis buffer after puromycin selection. HSC70 was used as loading control for the quantification of FASN expression. The western blot is shown on the left and the statistic results on the right. Analysis is shown on the right side with y axis of fold change normalized to the expression level of FASN in scr. Each sample was loaded 3 times and analyzed by t test. Significance is presented in the graphs as * for $p < 0.05$.

After the establishment of the stable FASN knockdowns in Kasumi cells, the biological effect of FASN knockdown on the levels of fatty acids was analyzed in Kasumi cells by chromatography experiments which were performed by Dr. Anna Worthmann in the laboratory of Prof. Dr. Jörg Heeren. After chromatography of the Kasumi cell extracts, 27 fatty acids were detected and their levels were quantified. In figure 2 the relative amount of each fatty acid is shown in Kasumi cells after knockdown of FASN (kd1 and kd2) normalized to Kasumi1 cells without knockdown (scr). An overall reduction in palmitic acid levels confirm the successful knockdown of FASN in Kasumi1 cells.

A

Cell line	phenotype	palmitic acid (ug/ul)	palmitic acid (%)	FASN (%)
Kasumi1	SCR	188,219	100.00%	100,00%
Kasumi1	FASN-KD1	83,1075	44.15%	19,33%
Kasumi1	FASN-KD2	60,8425	32.33%	14,60%

Relative palmitic acid amounts (%)

B

Myristolic acid (C14:0)

Myristoleic acid (C14:1)

plamitic acid C16:0

7-Hexadecenoic acid C16:1 (n-9)

Palmitoleic acid C16:1 (n-7)

Stearic acid C18:0

oleic acid C18:1

Vaccenic acid C18:1 n7

Linoleic acid C18:2 n-6

C

gLinoleneic acid C18:3 n6

aLinolenic acid C18:3 n3

Stearidonic acid C18:4 n3

Arachidic acid C20:0

Eicosanoic acid C20:1 n9

11-14-Eicosadienoic acid C20:2 n6

Dihomo-gamma-linolenic acid C20:3 n6

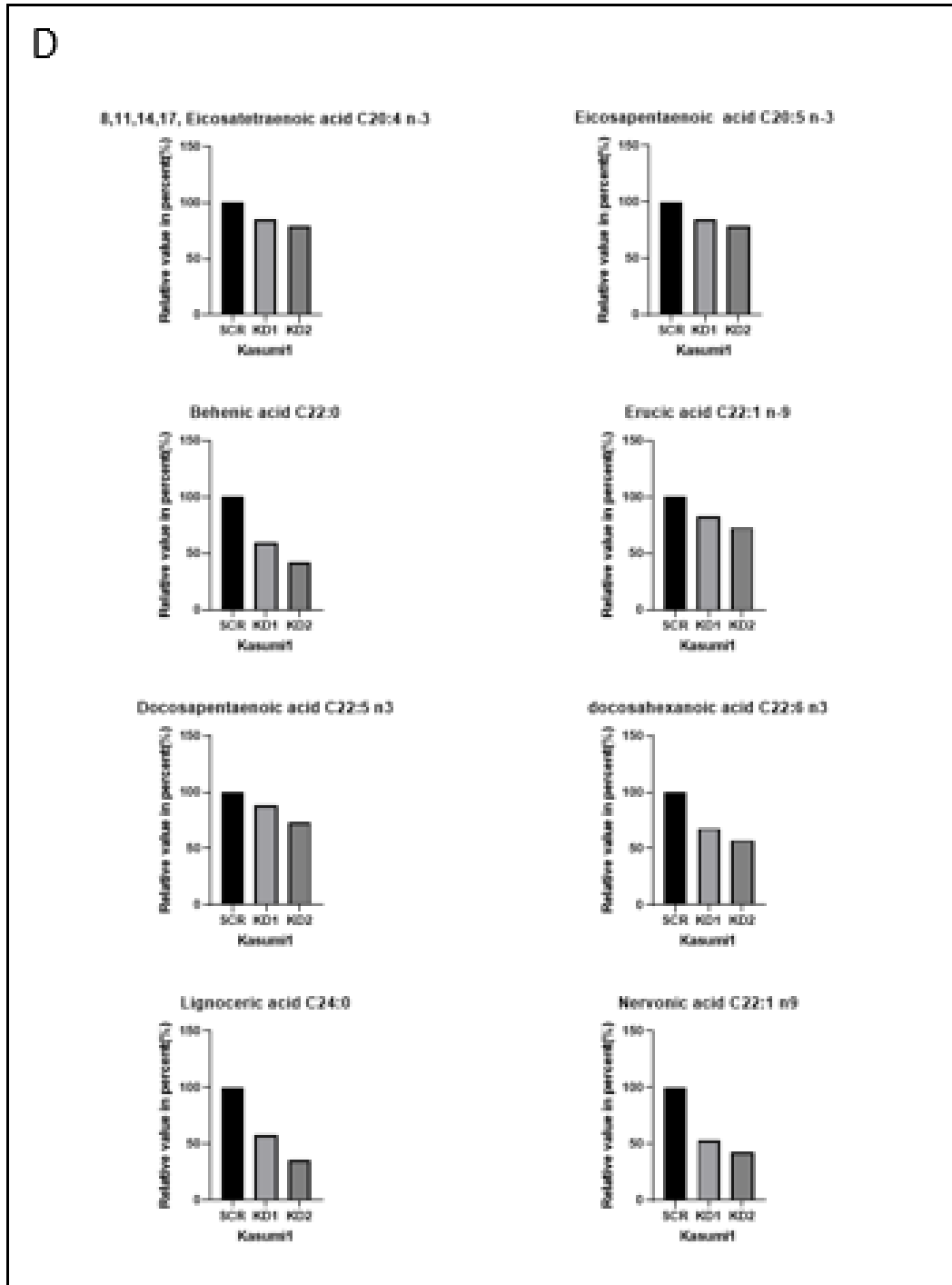Arachidonic acid C20:4 n-6

11,14,17, Eicosatrienoic acid C20:3 n-3

Figure 2

Lipidomic analysis of Kasumi1 cells: (A) Palmitic acid levels after knockdown of FASN in Kasumi1 cells. (B-D) Additional lipid acids were anaylsed in Kasumi1 cells after lentiviral-transduced knockdown of FASN by liquid chromatography.
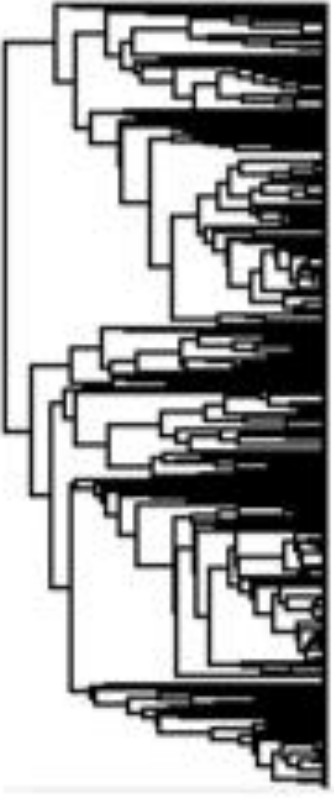
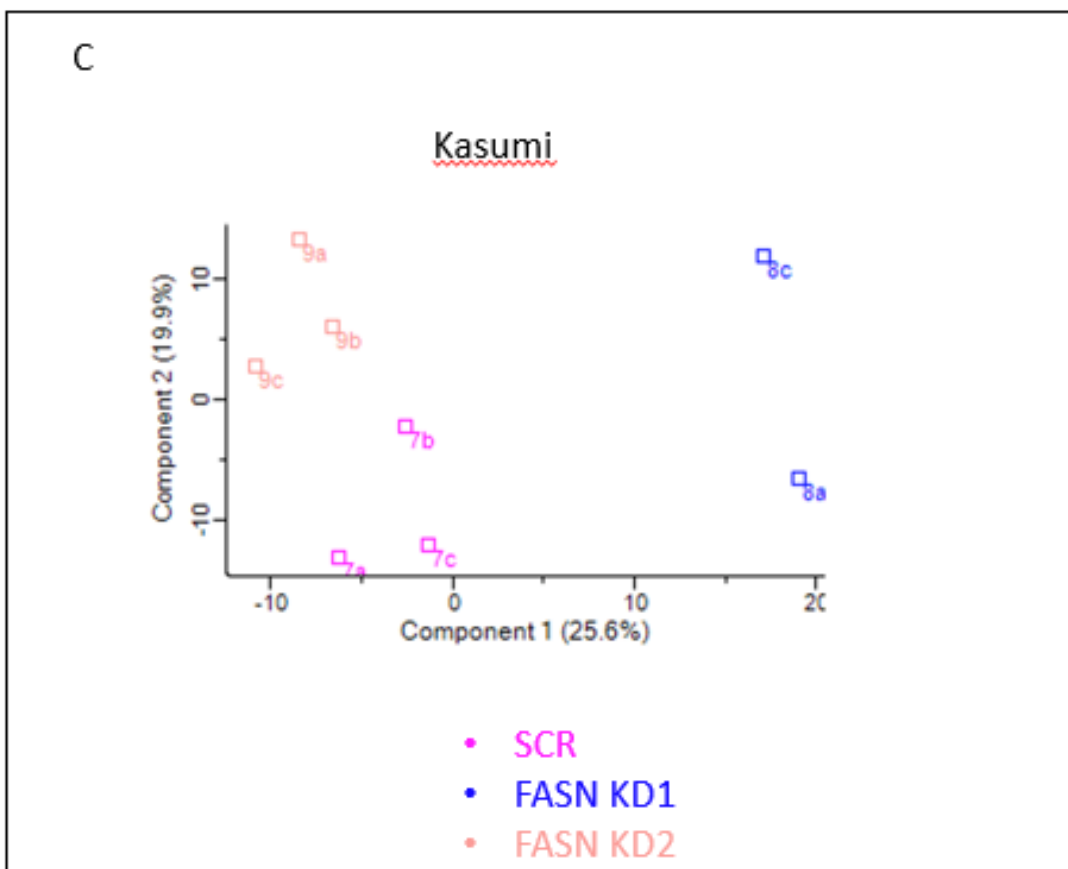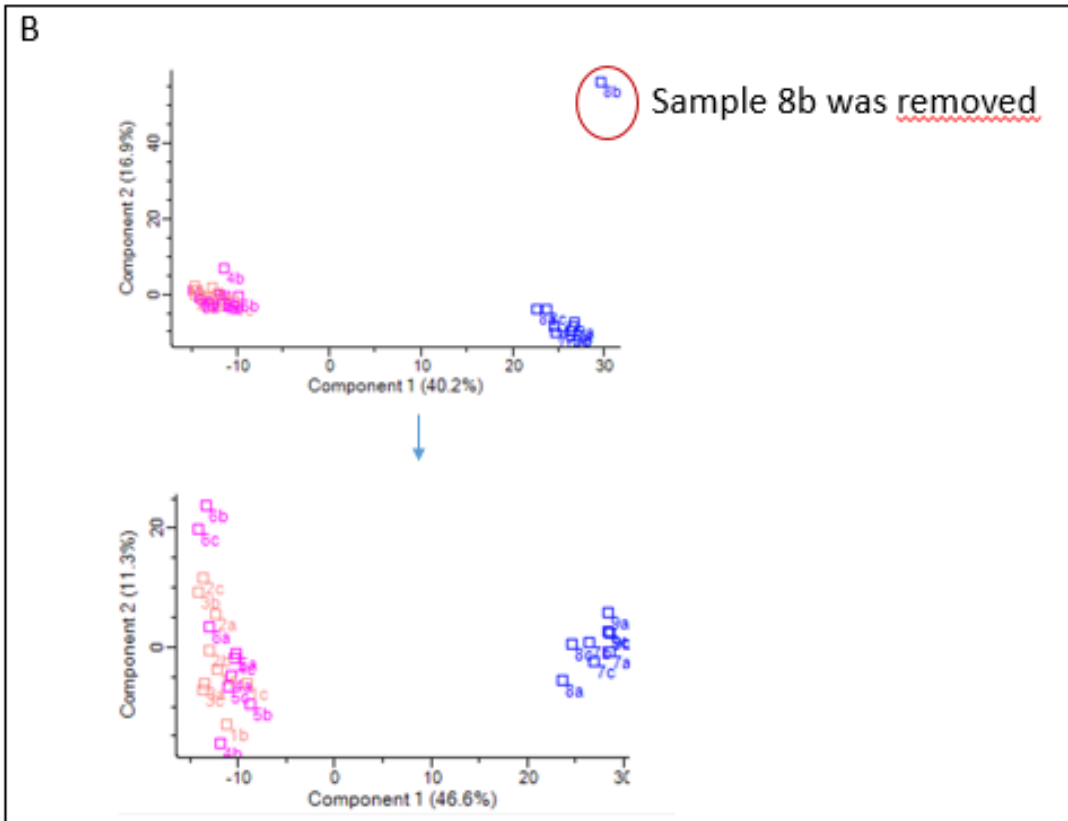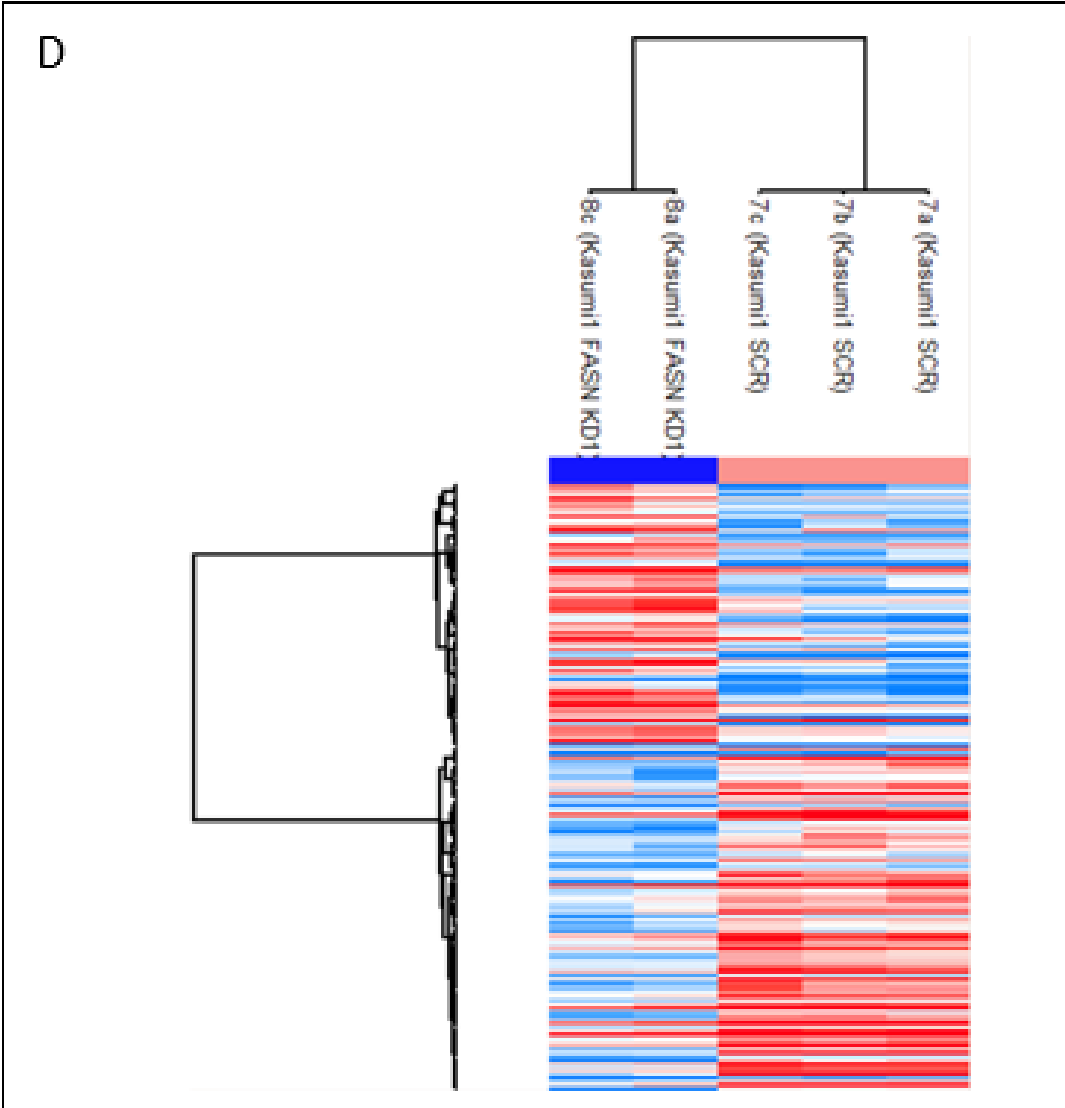In the next experiments, the proteins regulated by FASN knockdowns were

analysed by mass spectrometry (Fig. 4A-G). Two proteins, VPS45 and FASN, were found to be downregulated in both Kasumi1 FASN KD1 and Kasumi1 FASN KD2, compared with Kasumi1 SCR (Fig. 4H). Five proteins, PSMC4, SNRPG, GPX7, PDF and NEB, were found to be upregulated in both Kasumi1 FASN KD1 and Kasumi1 FASN KD2, compared with Kasumi1 SCR (Fig. 4I).

A

B

Sample 8b was removed

C

Kasumi

- SCR
- FASN KD1
- FASN KD2

E

FASN fold-change = -3.6 (downregulated)

Volcano Plot

F

G

FASN fold-change = -1.5 (downregulated)

Volcano Plot
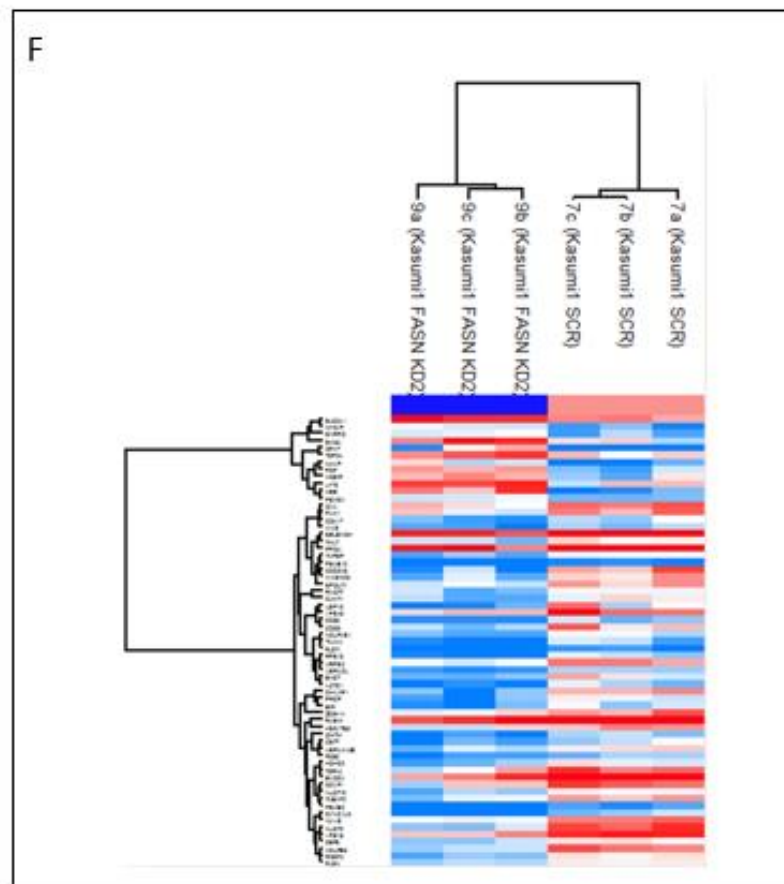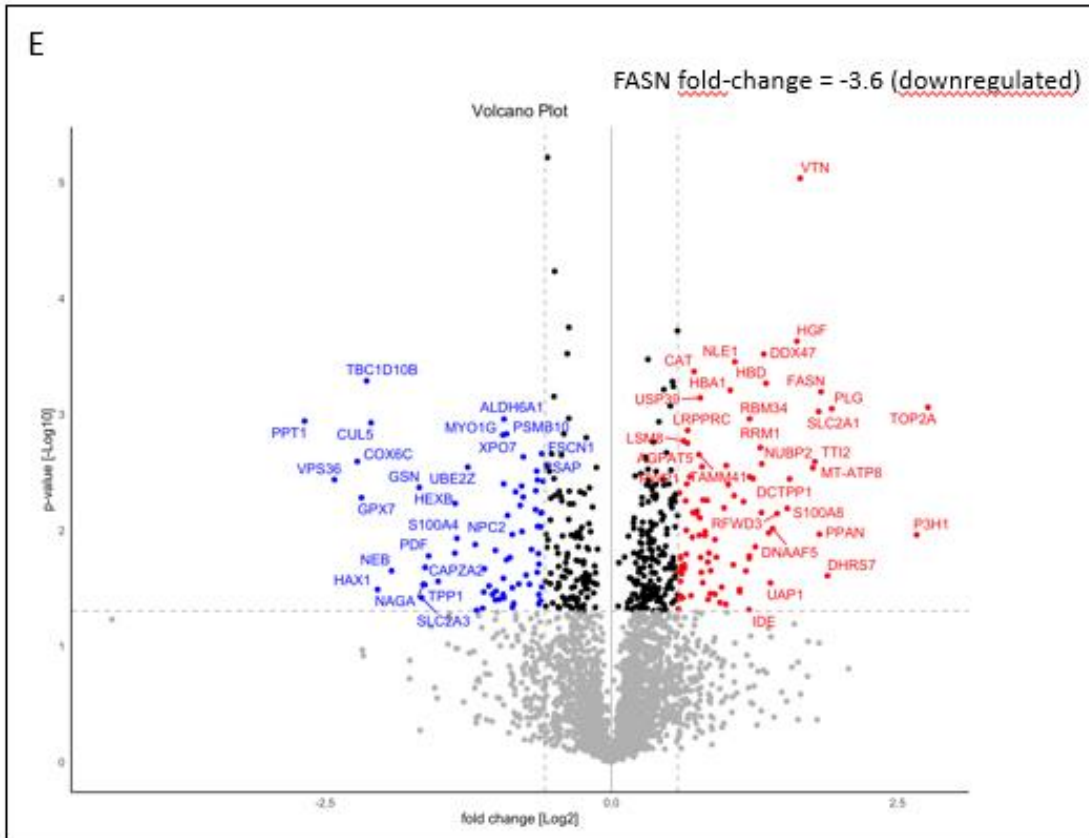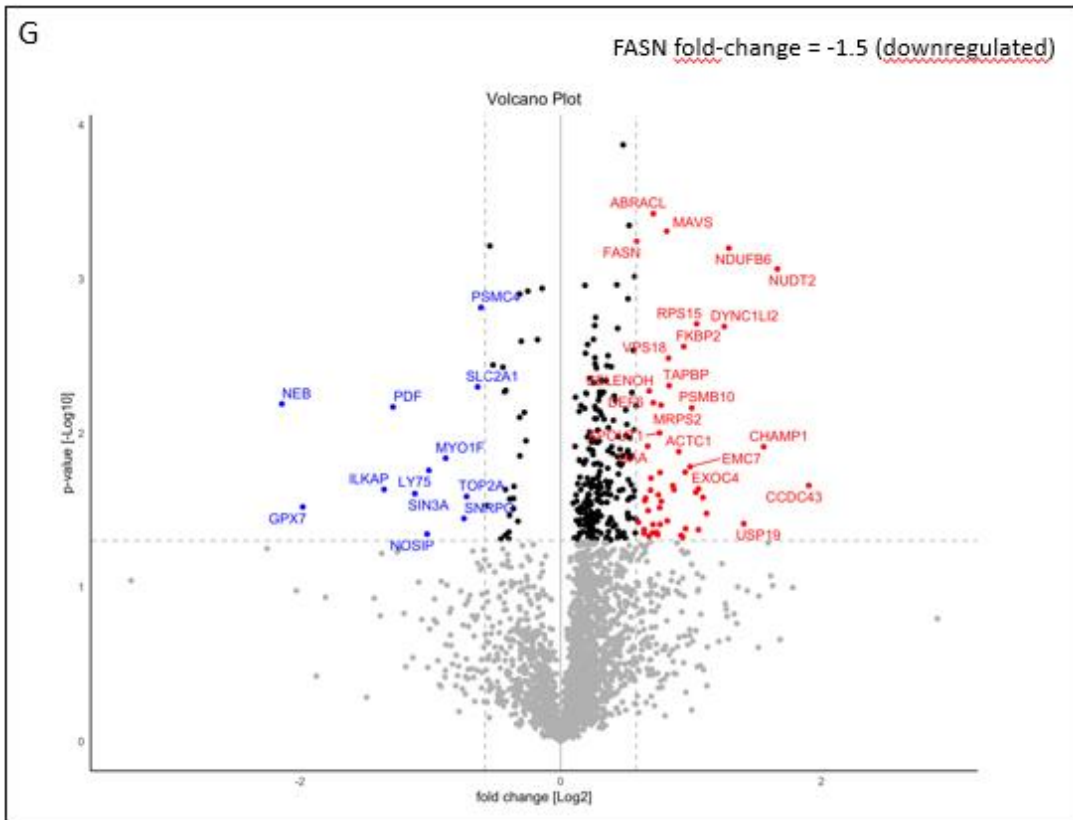
H

Lower abundant in KD cells
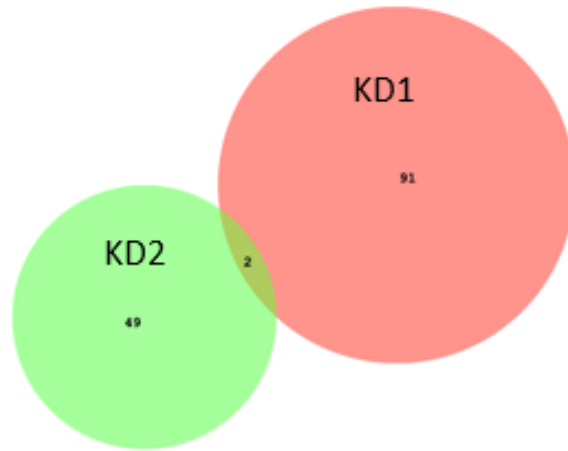
Protein overlap	Fold change KD 1	Fold change KD2
VPS45	-2	-1.6
FASN	-3.6	-1.5

Higher abundant in KD cells

Protein overlap	Fold change KD 1	Fold change KD2
PSMC4	1.8	1.5
SNRPG	2.2	1.7
GPX7	4.5	3.9
PDF	3.0	2.4
NEB	3.8	4.4

Figure 3

Identifications of FASN regulated protein expression by mass spectrometry-based proteomics.

Mass spectrometry and the subsequent analysis were performed by Hannah Voss and Bente Katharina Siebels. (A) Heat-map visualization of hierarchical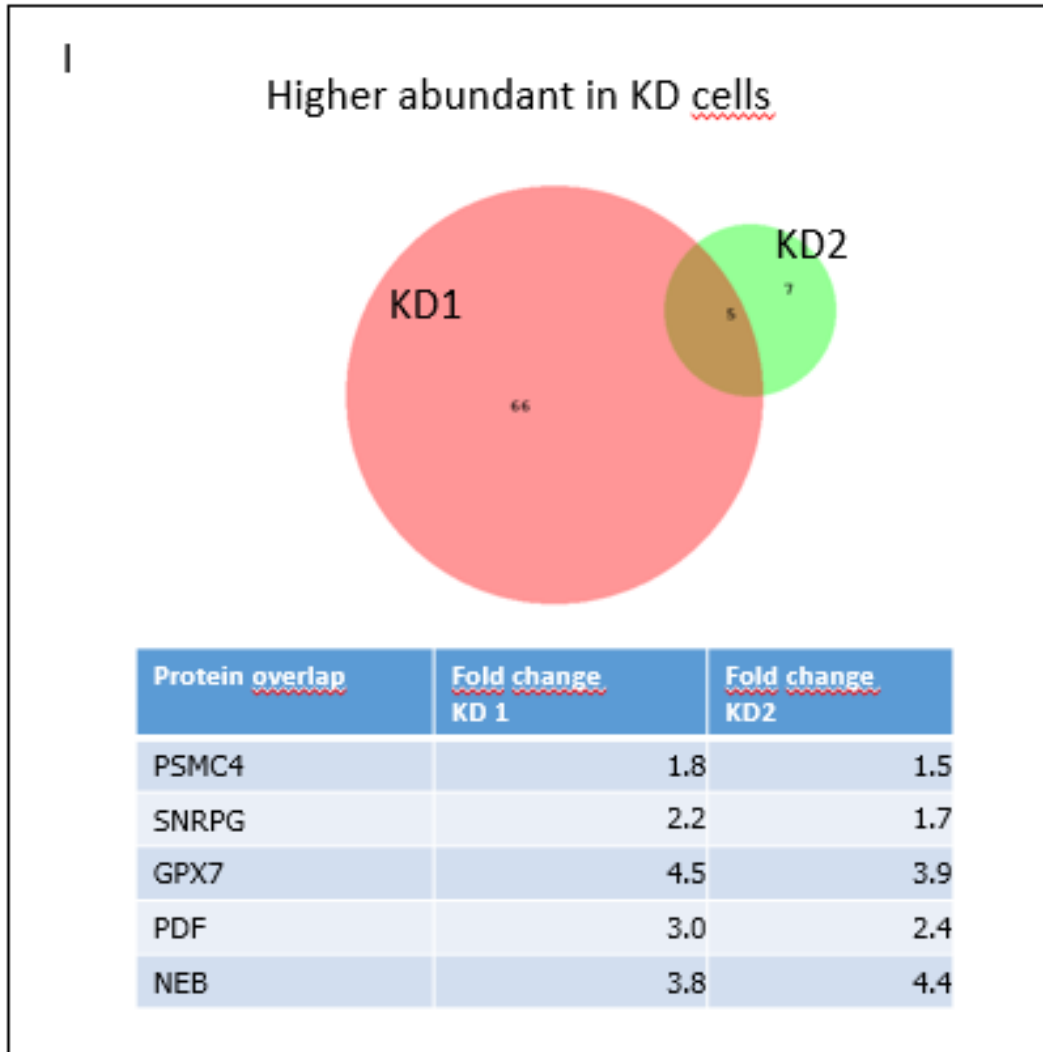 clustering based on Pearson correlation. Protein abundances were log 2 transformed and median normalized across columns. For better visualization abundances were mean normalized across rows. (B) Scatter plot visualization of principle component analysis (PCA) components 1 and 2. Sample 8b was removed because it is too different from the other two samples of the triplicate. (C) Scatter plot visualization of principle component analysis (PCA) components 1 and 2. (D-E) 164 proteins are significantly differential abundant between Kasumi1 SCR and Kasumi1 FASN KD1 in Student's t-test (p-value< 0.05, >1.5-fold change). (F-G) 63 proteins are significantly differential abundant between Kasumi1 SCR and Kasumi1 FASN KD2 in Student's t-test (p-value< 0.05, >1.5-fold change). (H) Venn Diagramm representing the overlap of siginificantly differential abundant proteins

(p-value<0.05, fold change >1.5) that are lower abundant in KD1 and KD2 Kasumi1 cells (SCR vs KD). (I) Venn Diagramm representing the overlap of siginificantly differential abundant proteins (p-value<0.05, fold change >1.5) that are higher abundant in KD1 and KD2 Kasumi1 cells (SCR vs KD).

In the next experiments, the impact of FASN specific knock down on expression and activation of proteins of the main effectors of PI3K/AKT/mTOR signaling pathway and RAS/MAPK signaling pathway was analysed by Western Blot (Fig. 4). An upregulation of standardized phosphorylation of S6 was observed in both Kasumi1 kd1 and Kasumi1 kd2 cells. As mentioned above, both PI3K/AKT/mTOR signaling pathway and RAS/MAPK signaling pathway can activate p70S6K and its downstream substrate S6. However, neither the PI3K/AKT pathway nor the RAS/MAPK pathway was changed in Kasumi1 FASN knockdown cells as demonstrated by unchanged levels of phosphoAKT and phosphoMAPK (Fig. 4).
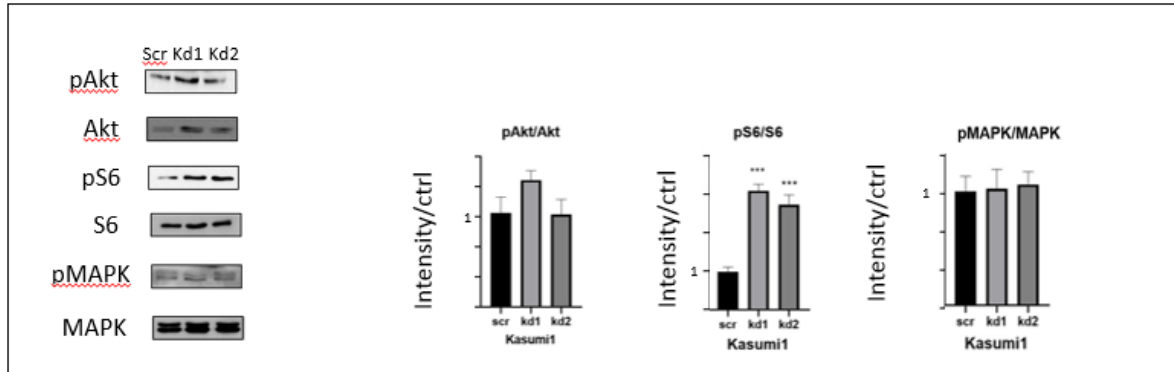
Figure 4

Increased phosphorylation of S6 after Knockdown of FASN in Kasumi1 cells.
Western blots were performed with whole cell lysates after stable knockdowns of Kasumi1 cells kd1 and kd2 and scr control cells. Samples were analyzed in technical triplicates. One of each of the three triplicates are shown on the left and the statistic results are shown on the right. Statistic bar charts used the optical density that were normalized to scr. Significance is presented in the graphs as * for p<0.05, ** for p<0.005, *** for p<0.001.

In order to analyze whether the upregulation of phosphorylation of S6 can also be

observed after inhibition of FASN with an inhibitor, Kasumi1 parental cells were treated with FASN inhibitor TVB3166 100nM at different time points. pS6 was found to be upregulated after 4 h and 8 h after treatment with the FASN inhibitor but was not detectable after 24 h of treatment (Fig. 5).

Figure 5 Increased phosphorylation of S6 after treatment of Kasumi1 cells with FASN inhibitor TVB3166. Kasumi1 parental cells were incubated with 100nM TVB3166 for 0h, 4h, 8h, and 24h. Whole cell lysates were collected at the indicated time points. Protein lysates were analysed for expression of phospho-S6 (pS6) and total S6 (S6) protein by western blots. Ponceau staining of the same membrane was used to demonstrate equal loading of protein lysates in each well which is shown beneath the western blots.

The upregulation of phospho-S6 after inhibition of Kasumi1 cells with the FASN inhibitor TVB3166 was analysed in an additional experiment which confirmed a statistical significant increase of phospho-S6 after 8 h of treatment (Fig. 6).
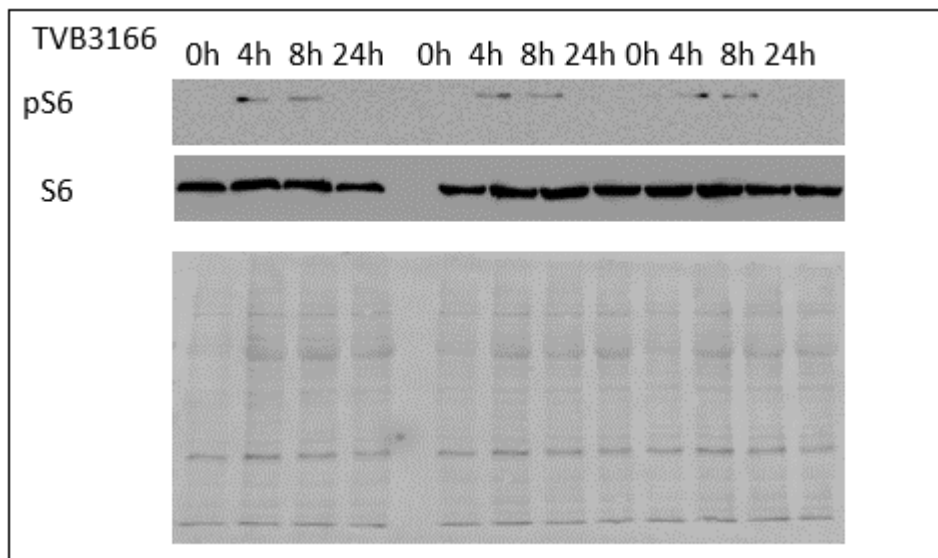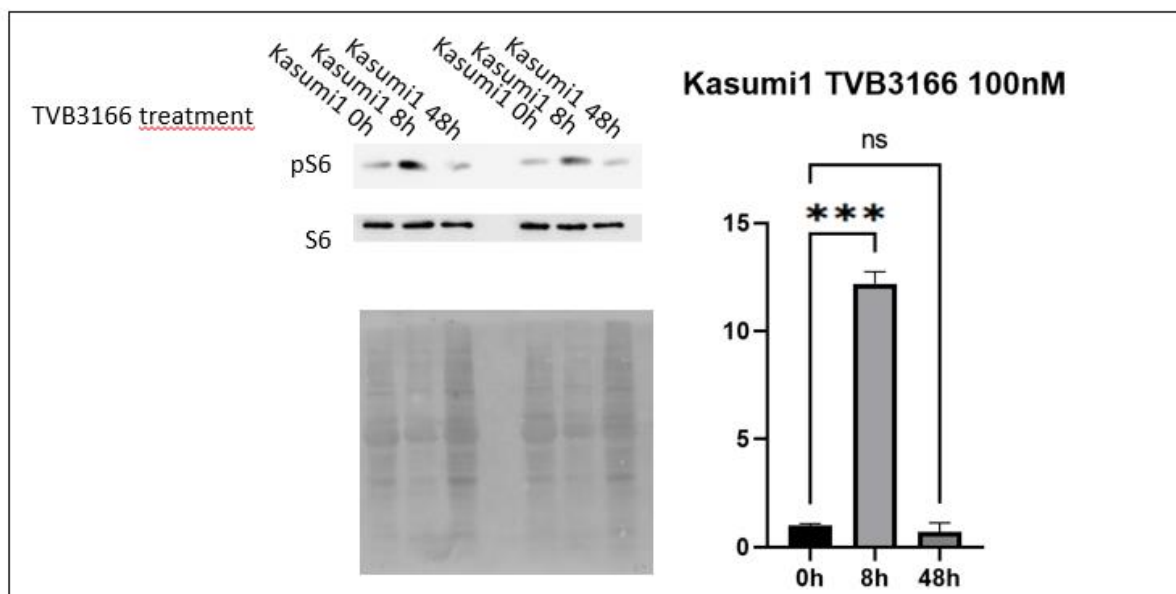
Figure 6 Increased phosphorylation of S6 after treatment with FASN inhibitor TVB3166.

Kasumi1 parental cells were incubated with 100nM TVB3166 for 0h, 8h, and 48h. Whole cell lysate were collected at the indicated time points. Protein lysates were analyzed for expression of pS6 and S6 with technical duplicates. Statistic bar charts used the optical density that were normalized to time 0h. Significance is presented in the graphs as *** = $p<0.001$.

In further experiments, the tyrosine kinases regulated by FASN in Kasumi1 cells were identified by kinome analysis. Expression of FASN was either reduced by knockdown or the activity of FASN was blocked by the FASN inhibitor TVB3166. As shown in figure 7, Lyn was upregulated in both Kasumi1 FASN knockdown1 and FASN knockdown2. Consistently, Lyn was also found to be upregulated when Kasumi1 cells were treated with 100nM FASN inhibitor TVB3166 for 5 days (Fig. 7).
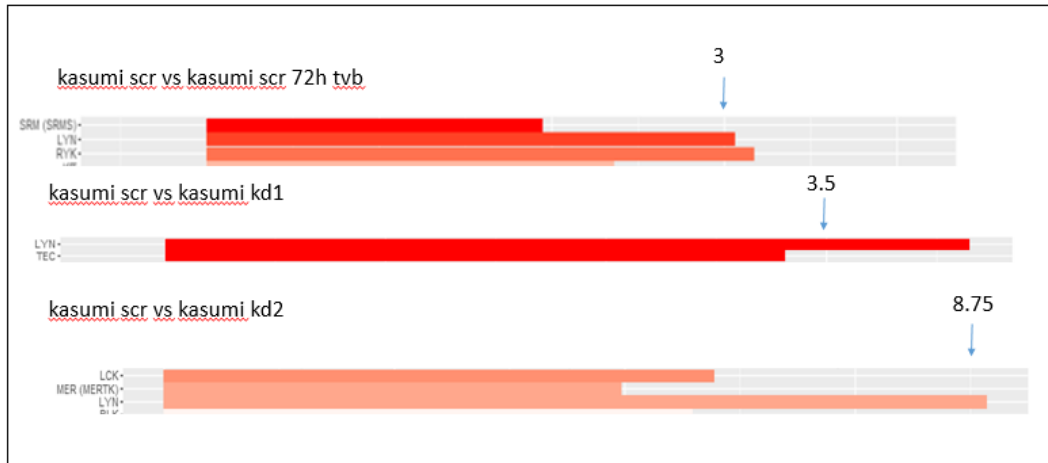
Figure 7. Kinome analysis of Kasumi1 cells. Kinome assays of Kasumi1 cells with FASN knockdowns (kd1 and kd2) or after blocking FASN activity with the inhibitor TVB3166 were performed by using PamChips for tyrosine kinases on a PamStation in the laboratory of Dr. Malte Kriegs (UKE). The indicated values written at the red bars indicate the log2 fold difference of Kasumi1 parental cells treated with FASN inhibitor relative to untreated control cells or after FASN knockdown relative tom scrambled control ells (scr). Only kinases regulated significantly are shown on the picture.

In order to confirm the observed upregulation of Lyn kinase after downregulation of FASN expression, the phosphorylation of Lyn kinase was analysed in the two stable Kasumi1 FASN knockdown cell lines kd1 and kd2 by western blots. As shown in figure 8, an increase of phospho-Lyn was observed in both FASN Kasumi1 knockdowns. However, the effect was not statistically significant.
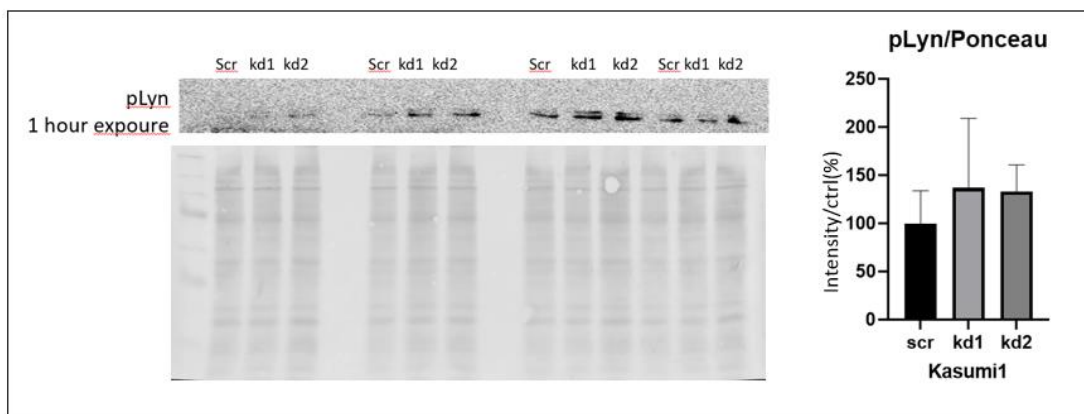
Figure 8. Increased phossphorylation of S6 in Kasumi1 FASN knockdown cells. pLyn was detected by western blot with whole cell lysate in technical triplicates by western blot analysis. Statistic bar charts used the optical density that were normalized to scr control cells.

In the next experiments the effect of FASN on proliferation of Kasumi1 cells was analysed. As shown in figure 9, there was no significant change of the proliferation of Kasumi1 cells after FASN knockdown or after treatment with100nM FASN inhibitor TVB3166.
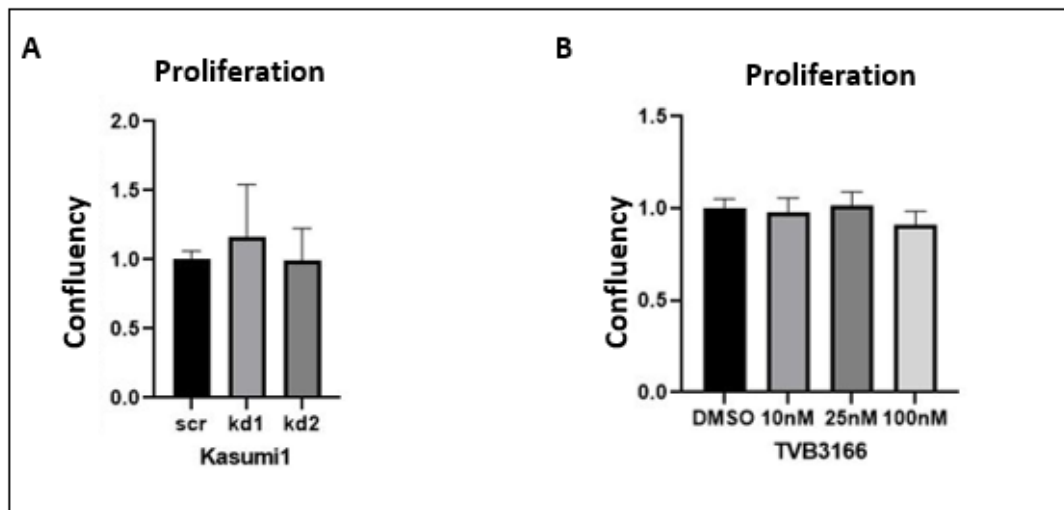
Figure 9. Proliferation of Kasumi1 cells after knockdown of FASN or inhibition of FASN activity.
(A) Proliferation of Kasumi1 SCR, Kasumi1 FASN knockdown1 (kd1) and Kasumi1 FASN knockdown2 (kd2) was analyzed by live cell imaging in an IncuCyte Zoom system. (B) Proliferation of Kasumi1 parental cells was analyzing by IncuCyte live cell imaging system after treatment with either DMSO or different concentrations of FASN inhibitor TVB3166.

4 Discussion

The goal of this thesis was the analysis of the functional role of fatty acid synthase (FASN) for the regulation of protein expression, kinase activity and signal transduction in AML cells. The AML cell line Kasumi1 was used as a model of AML. This cell line is derived from an AML patient with mutated c-KIT.

The protein known as tyrosine-protein kinase KIT, CD117 (cluster of differentiation 117), or mast/stem cell growth factor receptor (SCFR) is encoded by the proto-oncogene c-KIT (Andre et al., 1997). A heterodimer protein complex called core binding factor (CBF) is involved in the transcriptional control of the normal hematopoietic process. CBF is often altered in human leukemia and is required for the generation of hematopoietic stem cells (HSCs) during embryonic development. 20% of all adult AML are caused by molecular abnormalities of CBF (Sinha et al., 2015). According to cellular genetic and molecular anomalies, the European Leukemia Net (ELN) divides acute myeloid leukemia (AML) into favorable, moderate, and poor risk categories. According to this system of categorization, CBF AML, which is linked to CBF gene aberration, is a kind of acute myeloid leukemia with a favorable prognosis (Döhner et al., 2022; O'Donnell et al., 2017). The complete remission (CR) rate was 87-88%, while the relapse-free survival (RFS) rate was only 42% in a 10-year follow-up analysis with CBF AML (Appelbaum et al., 2006). The KIT gene is the most often altered (15–45%) in CBF-AML. The type III tyrosine kinase family is represented by the 145-kDa transmembrane glycoprotein encoded by the KIT gene, which is found on chromosomal band 4q11–12. When stem cell factor (a KIT ligand) binds to the KIT receptor, it opens up signaling pathways that are crucial for cell growth, differentiation, and survival (Malaise et al., 2009). Exon 8 and the tyrosine kinase domain (exon 17) of the receptor are most frequently affected by KIT mutations, which cause ligand-independent activation. Exons 10 and 11 of the juxta-membrane domain are less often affected by mutations. KIT mutations are

linked to a poor prognosis in CBF-AML (Pollard et al., 2010).

The functional role of FASN is to catalyze the synthesis of fatty acids (Jensen-Urstad and Semenkovich, 2012). It was discovered in mammary glands during lactation, and other lipogenic tissues such as the liver and adipose tissue (Swierczyński and Sledziński, 2012). Fatty acid synthase is a crucial enzyme in the production of fatty acids in animals and its activities is affected by nutritional manipulations (Donaldson, 1979). As a reversible post-translational lipid modification, palmitoylation—also known as S-palmitoylation or S-acylation—involves the covalent attachment of a long-chain fatty acid, often the 16-carbon palmitate, to one or more cysteine residues throughout the protein via a thioester bond (Li and Qi, 2017).

In order to analyze the functional role of FASN in human AML cells, stable knockdowns of FASN were made successfully by lentiviral transduction with two FASN-shRNA vectors in Kasumi1 cells. The FASN knockdown was confirmed in both Kasumi1 kd cell lines by western blots. Lipidomic anaylsis confirmed the reduction of palmitic acid as well as several other fatty acids in Kasumi1 FASN knockdown cells. Moreover, mass spectrometry-based proteomics analysis also confirmed the reduced expression of FASN in Kasumi1 FASN knockdown1 and Kasumi1 FASN knockdown2 cells in comparison to SCR control cells. In addition to FASN, VPS45 was also found to be downregulated in both FASN knockdown Kasumi1 cells. VPS45 is the short term for Vacuolar Protein Sorting 45 Homolog. Although its precise function is unknown, considering that protein sorting by vesicles is crucial for the division of intracellular molecules into various organelles, this gene's high level of expression in peripheral blood mononuclear cells implies that it may play a role in the transportation of proteins, including inflammatory mediators (provided by RefSeq, Jul 2013). So far, there is no reliable data to prove the relationship between VPS45 and FASN. In addition, 5 proteins, PSMC4, Small Nuclear Ribonucleoprotein Polypeptide G (SNRPG), Glutathione Peroxidase 7 (GPX7), Peptide Deformylase (PDF) and Nebulin (NEB), were found to be

upregulated in Kasumi1 FASN knockdown1 and knockdown2.

PSMC4, is the gene encoding component of the 26S proteasome, which is a multiprotein complex involved in the ATP-dependent degradation of ubiquitinated proteins. This complex plays a key role in the maintenance of protein homeostasis by removing misfolded or damaged proteins, which could impair cellular functions, and by removing proteins whose functions are no longer required. (PRS6B_HUMAN,P43686).

SNRPG encodes a component of the U1, U2, U4, and U5 small nuclear ribonucleoprotein complexes, precursors of the spliceosome. As part of the U7 snRNP it is involved in histone 3'-end processing. (RUXG_HUMAN,P62308).

Protein encoded by GPX7 protects esophageal epithelia from hydrogen peroxide-induced oxidative stress. It suppresses acidic bile acid-induced reactive oxigen species (ROS) and protects against oxidative DNA damage and double-strand breaks. (GPX7_HUMAN,Q96SL4). Interestingly, GPx7 may be a potential therapeutic target to stop the progression and onset of non-alcoholic fatty liver disease (NAFLD), according to a number of in vitro and in vivo studies (Kim et al., 2020). Unfortunately, no study has shown so far that GPx7 plays a similar function as a tumor suppressor in leukemia.

In eubacteria and eukaryotic organelles, peptide deformylase (PDF) removes the formyl group from the initiating methionine of nascent peptides. In eubacteria, deformylation of nascent peptides is required for subsequent cleavage of initiating methionines by methionine aminopeptidase. The discovery that a natural inhibitor of PDF, actinonin, acts as an antimicrobial agent in some bacteria has spurred intensive research into the design of bacterial-specific PDF inhibitors. In human cells, only mitochondrial proteins have N-formylation of initiating methionines. Protein inhibitors of PDF or siRNAs of PDF block the growth of cancer cell lines but have no effect on normal cell growth. In humans, PDF function may therefore be restricted to rapidly growing cells. (provided by RefSeq, Nov 2008).

Nebulin, a giant protein component of the cytoskeletal matrix that coexists with the thick and thin filaments within the sarcomeres of skeletal muscle. In most vertebrates, nebulin accounts for 3 to 4% of the total myofibrillar protein. This protein contains approximately 30-amino acid long modules that can be classified into 7 types and other repeated modules. It may be involved in maintaining the structural integrity of sarcomeres and the membrane system associated with the myofibrils. It also binds and stabilize F-actin. (NEBU_HUMAN,P20929).

In addition, the role of FASN for the regulation of distinct signaling pathways which are often activated in AML cells i.e. the PI3K/AKT/mTOR and RAS/RAF/MEK/MAPK pathways was analysed. Intriguingly, as shown in the western blot results in figure 4, S6 activation by phosphorylation was significantly elevated in both FASN knockdown1 and knockdown2 Kasumi1 cells. Consistently, this upregulation in S6 activation was also demonstrated by using an FASN inhibitor. In order to find a possible explanation behind the mechanism of activation of p70S6 kinase signaling, Kinome assays of the Kasumi1 cells with FASN knockdowns were performed by using PamChips for tyrosine kinases on a PamStation in the laboratory of Dr. Malte Kriegs (UKE). The results suggested that Lyn was upregulated in both Kasumi1 FASN knockdown1 cells and Kasumi1 FASN knockdown2 cells. In accordance with the Pamgene data, the level of pLyn showed the same upregulation tendency in Kasumi1 parental cells treated with FASN inhibitor. The quantification analysis confirmed that pLyn was upregulated in both FASN knockdown Kasumi1 cells, but this change was not significantly.

Lyn, a member of the Src kinase family (SFK), was aimed to be inappropriately distributed throughout the plasma membrane and the cytoplasm in AML cells where it was expressed in an active state (Dos Santos et al., 2008). Lyn plays the role of a signaling component of the FLT3/ITD-specific pathway linking FLT3/ITD to STAT5 by binding itself to FLT3/ITD receptor. The upregulation of Lyn in the context of FASN knockdown in Kasumi1 cells has been confirmed by western blot, which correlates with the results of that in Kasumi1 parental cells treated with FASN

inhibitor TVB3166. In a recent study, it has been shown that Lyn is important for the delivery of fatty acids into adipocytes and interestingly, this process is dependent on the dynamic palmitoylation of CD36 (Hao et al., 2020). As for AML, Lyn is indicated to be a regulator of Acetyl-CoA-mediated metabolic pathways in which a Lyn inhibitor can reduce the Acetyl-CoA synthesis (Basappa et al., 2020). In this thesis, Lyn was found to be upregulated after FASN knockdown, which could be an explanation of the accumulation of Acetyl-CoA reserved from the suppressed process of fatty acid synthesis mediated by reduced FASN. On the other hand, the activation of S6 seems to be time course dependend, which means, according to the above-mentioned results, the upregulation of pS6 has a determined time window of several hours, and the effect was already unable to be detected after treating with FASN inhibitor for 24h. While considering the upregulation of pLyn that has been detected in both stable-transduced FASN knockdown Kasumi1 cells (by western blot) and in the Kasumi1 parental cells using FASN inhibitor for 5 days (by using PamChips), it seems that the activation of Lyn is more stable over a long time period. Even though, there's still the possibility that Lyn and pS6 are regulated in certain patterns. As it was stated in a publication in 2006, specific downregulation of Lyn by the method of si-RNA resulted in a significant reduction in the phosphorylation of p70S6K (Recher et al., 2006). These data as well as the results obtained in this thesis regarding the regulation of both Lyn and p70S6K either by using FASN inhibitor or reduced expression of FASN strongly suggest a direct functional role of FASN in the regulation of Lyn kinase for the upregulation of phospho-S6. Therefore, it is worth to analyse the role of a putative Lyn-mediated upregulation of pS6 after FASN knockdown in more

detail. This will give us more information regarding the regulation between FASN, Lyn and S6. As mentioned before, activation of S6 could be the result from its upstream signaling PI3K-AKT-mTor pathway or RAS-MAPK pathway. However, since no significant change in activation of AKT or MAPK was detected while pS6 was upregulated, another signaling pathway is most likely responsible for the effect

on pS6 upregulation after FASN downregulation.

A possible mechanism that are responsible for the observed activation of S6 after FASN knockdown could be the Rho Family G Proteins Cdc42 and Rac1. It was demonstrated that Rac1, Cdc42 and inactive p70S6K can form a complex. This kind of complex can activate p70S6K through the dynamic process of Rac1-GDP to Rac1-GTP conversion. These could be a parallel signal mediated by PI3K (Chou and Blenis, 1996). In this case, it could be interesting to further investigate the function of Rac1 or the activation of p70S6K kinase activation. Potential methods include detection of the activity of p70S6K kinase after knockdown or silencing of Rac1 in FASN knockdown cells. There are additional kinases which have been described to be involved in the phosphorylation of S6 like p90 rpS6K (RSK), protein kinase A (PKA), Casein kinase 1 (CK1) and phosphoinositide-dependent kinase 1 (PDK1) which can also phosporylate S6 (Meyuhas, 2015). However, the phosphorylation by these kinases occur at other sites in S6 than S240/244 detected with the phospho-RPS6 antibody used in this study. Therefore, these kinases cannot be responsible for the FASN-mediated increase in p70S6K phosphorylation observed in this thesis.

The proliferation of Kasumi1 cells after lentiviral mediated FASN knockdown or FASN inhibitor did not change significantly. A publication in 2008 suggests that by using either a SFK inhibitor that has the ability to reduce tyrosine activation in a global level, or by silencing Lyn expression through siRNA, proliferation of AML patient cells were shown to be reduced in both situations (Dos Santos et al., 2008). However, this previous results don't correlate with the unchanged proliferation of Kasumi cells after FASN knockdown and Lyn activation that has been observed in this thesis. The functional role of FASN for proliferation of AML cells has to be analysed in further experiments.

5 Summary (English version)

Acute myeloid leukemia (AML) is the most common leukemia in adults and characterized by an uncontrolled proliferation of myeloid cells. Fatty acid synthase (FASN) is mediating the biosynthesis of fatty acids and its expression in AML cells is higher than in granulocytes and $CD34^+$ hematopoietic progenitor cells from healthy donors. However, the functional role of upregulated FASN on the regulation of signal transduction has not been analyzed in AML cells in detail. The purpose of this thesis was the analysis of the functional role of FASN for the regulation of protein expression, kinase activity and signal transduction in AML cells.

The AML cell line Kasumi1 was used as a model system to study the effect of FASN. Stable knockdowns of FASN were generated in Kasumi1 cells by two independent lentiviral shRNA vectors and a scramble shRNA vector as control. The successful FASN knockdown in Kasumi1 cells were confirmed by reduced levels of FASN in Kasumi1 knockdown cells by western blot and mass spectrometry. In addition, the levels of palmitic acid and several additional fatty acids were reduced in FASN knockdown cells as demonstrated by liquid chromatography experiments. The FASN-mediated regulation of protein expression analysed by mass spectrometry revealed a downregulation of VPS45 and FASN and an upregulation of PSMC4, SNRPG, GPX7, PDF and NEB in Kasumi1 cells after FASN knockdowns. A kinome profiling of Kasumi1 FASN knockdown cells was performed on a PamStation by using PamChips for tyrosine kinases and revealed an upregulation of the Src family member Lyn after FASN knockdown as well as after blocking FASN enzymatic activity with the FASN inhibitor TVB3166. In addition, the effects of the FASN knockdowns on signaling pathways were tested. Increased phosphorylation of Lyn and S6 were detected while neither PI3K/AKT pathway nor RAS/MAPK pathway was changed. The biological effect of FASN on cell growth was analyzed by live cell imaging using an IncuCyte Zoom system which did not reveal a significant change of the proliferation of Kasumi1 cells after FASN knockdown or after inhibition of the

enzymatic activity of FASN with TVB1366.

In further experiments, the functional role of the FASN-regulated expression of the identified proteins and the putative Lyn-mediated upregulation of pS6 after FASN knockdown have to be studied in more detail.

6 Zusammenfassung

Die akute myeloische Leukämie (AML) ist die häufigste Leukämie bei Erwachsenen und durch eine unkontrollierte Proliferation von myeloischen Zellen gekennzeichnet. Die Fettsäuresynthase (FASN) vermittelt die Biosynthese von Fettsäuren und ihre Expression ist in AML-Zellen höher als in Granulozyten und CD34+ hämatopoetischen Vorläuferzellen von gesunden Spendern. Die funktionelle Rolle von hochreguliertem FASN bei der Regulierung der Signaltransduktion wurde in AML-Zellen jedoch noch nicht im Detail untersucht. Das Ziel dieser Arbeit war die Analyse der funktionellen Rolle von FASN für die Regulation der Proteinexpression, Kinaseaktivität und Signaltransduktion in AML-Zellen.

Die AML-Zelllinie Kasumi1 wurde als Modellsystem verwendet, um die Wirkung von FASN zu untersuchen. Stabile Knockdowns von FASN wurden in Kasumi1-Zellen durch zwei unabhängige lentivirale shRNA-Vektoren und einen Scramble-shRNA-Vektor als Kontrolle erzeugt. Der erfolgreiche FASN-Knockdown in Kasumi1-Zellen wurde durch reduzierte FASN-Konzentrationen in Kasumi1-Knockdown-Zellen mittels Western Blot und Massenspektrometrie bestätigt. Darüber hinaus war der Gehalt an Palmitinsäure und verschiedenen anderen Fettsäuren in den FASN-Knockdown-Zellen reduziert, wie durch Flüssigchromatographie-Experimente nachgewiesen wurde. Die FASN-vermittelte Regulation der Proteinexpression, die mittels Massenspektrometrie analysiert wurde, ergab eine Herabregulierung von VPS45 und FASN und eine Hochregulierung von PSMC4, SNRPG, GPX7, PDF und NEB in Kasumi1-Zellen nach FASN-Knockdowns. Ein Kinom-Profiling von Kasumi1-Zellen mit FASN-Knockdown wurde auf einer PamStation unter Verwendung von PamChips für Tyrosinkinasen durchgeführt und zeigte eine Hochregulierung des Src-Familienmitglieds Lyn nach FASN-Knockdown sowie nach Blockierung der enzymatischen Aktivität von FASN mit dem FASN-Inhibitor

TVB3166. Darüber hinaus wurden die Auswirkungen der FASN-Knockdowns auf Signalwege getestet. Es wurde eine erhöhte Phosphorylierung von Lyn und S6 festgestellt, während weder der PI3K/AKT-Signalweg noch der RAS/MAPK-Signalweg verändert war. Die biologische Wirkung von FASN auf das Zellwachstum wurde mit Hilfe von Live-Cell-Imaging unter Verwendung eines IncuCyte-Zoom-Systems analysiert. Dabei wurde keine signifikante Veränderung der Proliferation von Kasumi1-Zellen nach FASN-Knockdown oder nach Hemmung der enzymatischen Aktivität von FASN mit TVB1366 festgestellt.

In weiteren Experimenten muss die funktionelle Rolle der FASN-regulierten Expression der identifizierten Proteine und die mutmaßliche Lyn-vermittelte Hochregulierung von pS6 nach FASN-Knockdown genauer untersucht werden.

7 Abbreviations

Acute Myeloid Leukemia (AML); cysteine at position 563 (C563); Core binding factor-AML (CBF-AML); CD117 (cluster of differentiation 117); complete remission (CR); diffuse large B-cell lymphoma (DLBCL); European Leukemia Net (ELN); RAS/extracellular signal–regulated kinase (ERK); Fatty Acid Synthase (FASN); FMS-like tyrosine kinase 3 (FLT3); Glutathione Peroxidase 7 (GPX7); Hedgehog (Hh); hematopoietic stem cells (HSCs); International Cancer Conference (ICC); Internal tandem duplication (ITD); juxtamembrane domain (JM domain); mitogen-activated protein kinase (MAPK); mantle cell lymphoma (MCL); Non-alcoholic fatty liver disease (NAFLD); Nebulin (NEB); Peptide Deformylase (PDF); primary exudative lymphoma (PEL); plasma membrane (PM); reactive oxigen species (ROS); patched homolog 1 (PTCH1); relapse-free survival (RFS); RPS6 (Ribosomal Protein S6); stem cell growth factor receptor (SCFR); stem cell transplant (SCT); Src family kinases (SFKs); Smoothened homolog (Smo); Small Nuclear Ribonucleoprotein Polypeptide G (SNRPG); suppressor of fused homolog (SuFu); tyrosine kinase domain (TKD); World Health Organization (WHO); wild-type (WT)

8   Reference list

Acute Myeloid Leukemia Treatment (PDQ®)–Patient Version - National Cancer Institute [WWW Document], 2022. URL https://www.cancer.gov/types/leukemia/patient/adult-aml-treatment-pdq (accessed 3.28.22).

Ahn, N.G., Weiel, J.E., Chan, C.P., Krebs, E.G., 1990. Identification of multiple epidermal growth factor-stimulated protein serine/threonine kinases from Swiss 3T3 cells. J. Biol. Chem. 265, 11487–11494.

An, W.-L., Cowburn, R.F., Li, L., Braak, H., Alafuzoff, I., Iqbal, K., Iqbal, I.-G., Winblad, B., Pei, J.-J., 2003. Up-Regulation of Phosphorylated/Activated p70 S6 Kinase and Its Relationship to Neurofibrillary Pathology in Alzheimer's Disease. Am. J. Pathol. 163, 591–607.

Andre, C., Hampe, A., Lachaume, P., Martin, E., Wang, X.P., Manus, V., Hu, W.X., Galibert, F., 1997. Sequence analysis of two genomic regions containing the KIT and the FMS receptor tyrosine kinase genes. Genomics 39, 216–226. https://doi.org/10.1006/geno.1996.4482

Appelbaum, F.R., Kopecky, K.J., Tallman, M.S., Slovak, M.L., Gundacker, H.M., Kim, H.T., Dewald, G.W., Kantarjian, H.M., Pierce, S.R., Estey, E.H., 2006. The clinical spectrum of adult acute myeloid leukaemia associated with core binding factor translocations. Br. J. Haematol. 135, 165–173. https://doi.org/10.1111/j.1365-2141.2006.06276.x

Arakawa, T., Yphantis, D.A., Lary, J.W., Narhi, L.O., Lu, H.S., Prestrelski, S.J., Clogston, C.L., Zsebo, K.M., Mendiaz, E.A., Wypych, J., 1991. Glycosylated and unglycosylated recombinant-derived human stem cell factors are dimeric and have extensive regular secondary structure. J. Biol. Chem. 266, 18942–18948.

Ayatollahi, H., Shajiei, A., Sadeghian, M.H., Sheikhi, M., Yazdandoust, E., Ghazanfarpour, M., Shams, S.F., Shakeri, S., 2017. Prognostic Importance of C-KIT Mutations in Core Binding Factor Acute Myeloid Leukemia: A Systematic Review. Hematol. Oncol. Stem Cell Ther. 10, 1–7. https://doi.org/10.1016/j.hemonc.2016.08.005

Basappa, J., Citir, M., Zhang, Q., Wang, H.Y., Liu, X., Melnikov, O., Yahya, H., Stein, F., Muller, R., Traynor-Kaplan, A., Schultz, C., Wasik, M.A., Ptasznik, A., 2020. ACLY is the novel signaling target of PIP2/PIP3 and Lyn in acute myeloid leukemia. Heliyon 6, e03910. https://doi.org/10.1016/j.heliyon.2020.e03910

Benjamin, D.I., Li, D.S., Lowe, W., Heuer, T., Kemble, G., Nomura, D.K., 2015. Diacylglycerol Metabolism and Signaling Is a Driving Force Underlying FASN Inhibitor Sensitivity in Cancer Cells. ACS Chem. Biol. 10, 1616–1623. https://doi.org/10.1021/acschembio.5b00240

Bhatt, A.P., Jacobs, S.R., Freemerman, A.J., Makowski, L., Rathmell, J.C., Dittmer, D.P., Damania, B., 2012. Dysregulation of fatty acid synthesis and glycolysis in non-Hodgkin lymphoma. Proc. Natl. Acad. Sci. 109, 11818–11823. https://doi.org/10.1073/pnas.1205995109

Bonner, T., O'Brien, S.J., Nash, W.G., Rapp, U.R., Morton, C.C., Leder, P., 1984. The human homologs of the raf (mil) oncogene are located on human chromosomes 3 and 4. Science 223, 71–74. https://doi.org/10.1126/science.6691137

Bonner, T.I., Kerby, S.B., Sutrave, P., Gunnell, M.A., Mark, G., Rapp, U.R., 1985. Structure and biological activity of human homologs of the raf/mil oncogene. Mol. Cell. Biol. 5, 1400–1407. https://doi.org/10.1128/mcb.5.6.1400-1407.1985

Boulton, T.G., Nye, S.H., Robbins, D.J., Ip, N.Y., Radziejewska, E., Morgenbesser, S.D., DePinho, R.A., Panayotatos, N., Cobb, M.H., Yancopoulos, G.D., 1991. ERKs: a family of protein-serine/threonine kinases that are activated and tyrosine phosphorylated in response to insulin and NGF. Cell 65, 663–675. https://doi.org/10.1016/0092-8674(91)90098-j

Broudy, V.C., Lin, N.L., Liles, W.C., Corey, S.J., O'Laughlin, B., Mou, S., Linnekin, D., 1999. Signaling via Src Family Kinases Is Required for Normal Internalization of the Receptor c-Kit. Blood 94, 1979–1986. https://doi.org/10.1182/blood.V94.6.1979

Cai, S.F., Levine, R.L., 2019. Genetic and epigenetic determinants of AML pathogenesis. Semin. Hematol., Advances in Acute Myeloid Leukemia 56, 84–89. https://doi.org/10.1053/j.seminhematol.2018.08.001

Carrière, A., Cargnello, M., Julien, L.-A., Gao, H., Bonneil, E., Thibault, P., Roux, P.P., 2008. Oncogenic MAPK signaling stimulates mTORC1 activity by promoting

RSK-mediated raptor phosphorylation. Curr. Biol. CB 18, 1269–1277. https://doi.org/10.1016/j.cub.2008.07.078

Chen, W.-L., Wang, J.-H., Zhao, A.-H., Xu, X., Wang, Y.-H., Chen, T.-L., Li, J.-M., Mi, J.-Q., Zhu, Y.-M., Liu, Y.-F., Wang, Y.-Y., Jin, J., Huang, H., Wu, D.-P., Li, Y., Yan, X.-J., Yan, J.-S., Li, J.-Y., Wang, S., Huang, X.-J., Wang, B.-S., Chen, Z., Chen, S.-J., Jia, W., 2014. A distinct glucose metabolism signature of acute myeloid leukemia with prognostic value. Blood 124, 1645–1654. https://doi.org/10.1182/blood-2014-02-554204

Choi, W.-I., Jeon, B.-N., Park, H., Yoo, J.-Y., Kim, Y.-S., Koh, D.-I., Kim, M.-H., Kim, Y.-R., Lee, C.-E., Kim, K.-S., Osborne, T.F., Hur, M.-W., 2008. Proto-oncogene FBI-1 (Pokemon) and SREBP-1 Synergistically Activate Transcription of Fatty-acid Synthase Gene (FASN). J. Biol. Chem. 283, 29341–29354. https://doi.org/10.1074/jbc.M802477200

Chou, M.M., Blenis, J., 1996. The 70 kDa S6 kinase complexes with and is activated by the Rho family G proteins Cdc42 and Rac1. Cell 85, 573–583. https://doi.org/10.1016/s0092-8674(00)81257-x

Crews, C.M., Erikson, R.L., 1992. Purification of a murine protein-tyrosine/threonine kinase that phosphorylates and activates the Erk-1 gene product: relationship to the fission yeast byr1 gene product. Proc. Natl. Acad. Sci. U. S. A. 89, 8205–8209. https://doi.org/10.1073/pnas.89.17.8205

Danilova, O.V., Dumont, L.J., Levy, N.B., Lansigan, F., Kinlaw, W.B., Danilov, A.V., Kaur, P., 2013. FASN and CD36 predict survival in rituximab-treated diffuse large

B-cell lymphoma. J. Hematop. 6, 11–18. https://doi.org/10.1007/s12308-012-0166-4

Döhner, H., Wei, A.H., Appelbaum, F.R., Craddock, C., DiNardo, C.D., Dombret, H., Ebert, B.L., Fenaux, P., Godley, L.A., Hasserjian, R.P., Larson, R.A., Levine, R.L., Miyazaki, Y., Niederwieser, D., Ossenkoppele, G., Röllig, C., Sierra, J., Stein, E.M., Tallman, M.S., Tien, H.-F., Wang, J., Wierzbowska, A., Löwenberg, B., 2022. Diagnosis and management of AML in adults: 2022 recommendations from an international expert panel on behalf of the ELN. Blood 140, 1345–1377. https://doi.org/10.1182/blood.2022016867

Donaldson, W.E., 1979. Regulation of fatty acid synthesis. Fed. Proc. 38, 2617–2621.

Dos Santos, C., Demur, C., Bardet, V., Prade-Houdellier, N., Payrastre, B., Récher, C., 2008. A critical role for Lyn in acute myeloid leukemia. Blood 111, 2269–2279. https://doi.org/10.1182/blood-2007-04-082099

Ferrari, S., Thomas, G., 1994. S6 phosphorylation and the p70s6k/p85s6k. Crit. Rev. Biochem. Mol. Biol. 29, 385–413. https://doi.org/10.3109/10409239409083485

Forte, D., García-Fernández, M., Sánchez-Aguilera, A., Stavropoulou, V., Fielding, C., Martín-Pérez, D., López, J.A., Costa, A.S.H., Tronci, L., Nikitopoulou, E., Barber, M., Gallipoli, P., Marando, L., Fernández de Castillejo, C.L., Tzankov, A., Dietmann, S., Cavo, M., Catani, L., Curti, A., Vázquez, J., Frezza, C., Huntly, B.J., Schwaller, J., Méndez-Ferrer, S., 2020. Bone Marrow Mesenchymal Stem Cells Support Acute Myeloid Leukemia Bioenergetics and Enhance Antioxidant

Defense and Escape from Chemotherapy. Cell Metab. 32, 829-843.e9. https://doi.org/10.1016/j.cmet.2020.09.001

Gelebart, P., Zak, Z., Anand, M., Belch, A., Lai, R., 2012. Blockade of Fatty Acid Synthase Triggers Significant Apoptosis in Mantle Cell Lymphoma. PLOS ONE 7, e33738. https://doi.org/10.1371/journal.pone.0033738

Ghaeidamini Harouni, M., Rahgozar, S., Rahimi Babasheikhali, S., Safavi, A., Ghodousi, E.S., 2020. Fatty acid synthase, a novel poor prognostic factor for acute lymphoblastic leukemia which can be targeted by ginger extract. Sci. Rep. 10, 14072. https://doi.org/10.1038/s41598-020-70839-9

Gilliland, D.G., Griffin, J.D., 2002. The roles of FLT3 in hematopoiesis and leukemia. Blood 100, 1532–1542. https://doi.org/10.1182/blood-2002-02-0492

Grafone, T., Palmisano, M., Nicci, C., Storti, S., 2012. An overview on the role of FLT3-tyrosine kinase receptor in acute myeloid leukemia: biology and treatment. Oncol. Rev. 6, e8. https://doi.org/10.4081/oncol.2012.e8

Griffith, J., Black, J., Faerman, C., Swenson, L., Wynn, M., Lu, F., Lippke, J., Saxena, K., 2004. The structural basis for autoinhibition of FLT3 by the juxtamembrane domain. Mol. Cell 13, 169–178. https://doi.org/10.1016/s1097-2765(03)00505-7

Gu, Y., Yang, R., Yang, Y., Zhao, Y., Wakeham, A., Li, W.Y., Tseng, A., Leca, J., Berger, T., Saunders, M., Fortin, J., Gao, X., Yuan, Y., Xiao, L., Zhang, F., Zhang, L., Gao, G., Zhou, W., Wang, Z., Mak, T.W., Ye, J., 2021. IDH1 mutation contributes to myeloid dysplasia in mice by disturbing heme biosynthesis and

erythropoiesis. Blood 137, 945–958. https://doi.org/10.1182/blood.2020007075

Hao, J.-W., Wang, J., Guo, H., Zhao, Y.-Y., Sun, H.-H., Li, Y.-F., Lai, X.-Y., Zhao, N., Wang, X., Xie, C., Hong, L., Huang, X., Wang, H.-R., Li, C.-B., Liang, B., Chen, S., Zhao, T.-J., 2020. CD36 facilitates fatty acid uptake by dynamic palmitoylation-regulated endocytosis. Nat. Commun. 11, 4765. https://doi.org/10.1038/s41467-020-18565-8

Hayakawa, F., Towatari, M., Kiyoi, H., Tanimoto, M., Kitamura, T., Saito, H., Naoe, T., 2000. Tandem-duplicated Flt3 constitutively activates STAT5 and MAP kinase and introduces autonomous cell growth in IL-3-dependent cell lines. Oncogene 19, 624–631. https://doi.org/10.1038/sj.onc.1203354

Heuer, T.S., Ventura, R., Mordec, K., Lai, J., Fridlib, M., Buckley, D., Kemble, G., 2017. FASN Inhibition and Taxane Treatment Combine to Enhance Anti-tumor Efficacy in Diverse Xenograft Tumor Models through Disruption of Tubulin Palmitoylation and Microtubule Organization and FASN Inhibition-Mediated Effects on Oncogenic Signaling and Gene Expression. EBioMedicine 16, 51–62. https://doi.org/10.1016/j.ebiom.2016.12.012

Hollander, M.C., Blumenthal, G.M., Dennis, P.A., 2011. PTEN loss in the continuum of common cancers, rare syndromes and mouse models. Nat. Rev. Cancer 11, 289–301. https://doi.org/10.1038/nrc3037

Jafari, N., Drury, J., Morris, A.J., Onono, F.O., Stevens, P.D., Gao, T., Liu, J., Wang, C., Lee, E.Y., Weiss, H.L., Evers, B.M., Zaytseva, Y.Y., 2019. De Novo Fatty Acid

Synthesis-Driven Sphingolipid Metabolism Promotes Metastatic Potential of Colorectal Cancer. Mol. Cancer Res. MCR 17, 140–152. https://doi.org/10.1158/1541-7786.MCR-18-0199

Jansen, H.W., Lurz, R., Bister, K., Bonner, T.I., Mark, G.E., Rapp, U.R., 1984. Homologous cell-derived oncogenes in avian carcinoma virus MH2 and murine sarcoma virus 3611. Nature 307, 281–284. https://doi.org/10.1038/307281a0

Jansen, H.W., Rückert, B., Lurz, R., Bister, K., 1983. Two unrelated cell-derived sequences in the genome of avian leukemia and carcinoma inducing retrovirus MH2. EMBO J. 2, 1969–1975.

Jensen-Urstad, A.P.L., Semenkovich, C.F., 2012. Fatty acid synthase and liver triglyceride metabolism: housekeeper or messenger? Biochim. Biophys. Acta 1821, 747–753. https://doi.org/10.1016/j.bbalip.2011.09.017

Jones, C.L., Stevens, B.M., D'Alessandro, A., Reisz, J.A., Culp-Hill, R., Nemkov, T., Pei, S., Khan, N., Adane, B., Ye, H., Krug, A., Reinhold, D., Smith, C., DeGregori, J., Pollyea, D.A., Jordan, C.T., 2018. Inhibition of Amino Acid Metabolism Selectively Targets Human Leukemia Stem Cells. Cancer Cell 34, 724-740.e4. https://doi.org/10.1016/j.ccell.2018.10.005

Kim, Hyeon Ju, Lee, Y., Fang, S., Kim, W., Kim, Hyo Jung, Kim, J.-W., 2020. GPx7 ameliorates non-alcoholic steatohepatitis by regulating oxidative stress. BMB Rep. 53, 317–322. https://doi.org/10.5483/BMBRep.2020.53.6.280

Koenig, K.L., Sahasrabudhe, K.D., Sigmund, A.M., Bhatnagar, B., 2020. AML with

Myelodysplasia-Related Changes: Development, Challenges, and Treatment Advances. Genes 11, E845. https://doi.org/10.3390/genes11080845

Kozak, C., Gunnell, M.A., Rapp, U.R., 1984. A new oncogene, c-raf, is located on mouse chromosome 6. J. Virol. 49, 297–299. https://doi.org/10.1128/JVI.49.1.297-299.1984

Lai, K.-O., Liang, Z., Fei, E., Huang, H., Ip, N.Y., 2015. Cyclin-dependent Kinase 5 (Cdk5)-dependent Phosphorylation of p70 Ribosomal S6 Kinase 1 (S6K) Is Required for Dendritic Spine Morphogenesis. J. Biol. Chem. 290, 14637–14646. https://doi.org/10.1074/jbc.M114.627117

Lennartsson, J., Blume-Jensen, P., Hermanson, M., Pontén, E., Carlberg, M., Rönnstrand, L., 1999. Phosphorylation of Shc by Src family kinases is necessary for stem cell factor receptor/c-kit mediated activation of the Ras/MAP kinase pathway and c-fos induction. Oncogene 18, 5546–5553. https://doi.org/10.1038/sj.onc.1202929

Linnekin, D., 1999. Early signaling pathways activated by c-Kit in hematopoietic cells. Int. J. Biochem. Cell Biol. 31, 1053–1074. https://doi.org/10.1016/S1357-2725(99)00078-3

Liu, K., 2006. Stem cell factor (SCF)-kit mediated phosphatidylinositol 3 (PI3) kinase signaling during mammalian oocyte growth and early follicular development. Front. Biosci.-Landmark 11, 126–135. https://doi.org/10.2741/1785

Long, R., Zhang, L., Shi, L., Shen, Y., Hu, F., Zeng, C., Min, W., 2017. Two-color vibrational imaging of glucose metabolism using stimulated Raman

scattering. Chem. Commun. 54, 152–155. https://doi.org/10.1039/C7CC08217G

Lv, K., Ren, J.-G., Han, X., Gui, J., Gong, C., Tong, W., 2021. Depalmitoylation rewires FLT3-ITD signaling and exacerbates leukemia progression. Blood 138, 2244–2255. https://doi.org/10.1182/blood.2021011582

Ma, L., Chen, Z., Erdjument-Bromage, H., Tempst, P., Pandolfi, P.P., 2005. Phosphorylation and functional inactivation of TSC2 by Erk implications for tuberous sclerosis and cancer pathogenesis. Cell 121, 179–193. https://doi.org/10.1016/j.cell.2005.02.031

Majumder, S., Brown, K., Qiu, F.H., Besmer, P., 1988. c-kit protein, a transmembrane kinase: identification in tissues and characterization. Mol. Cell. Biol. 8, 4896–4903. https://doi.org/10.1128/mcb.8.11.4896-4903.1988

Malaise, M., Steinbach, D., Corbacioglu, S., 2009. Clinical implications of c-Kit mutations in acute myelogenous leukemia. Curr. Hematol. Malig. Rep. 4, 77–82. https://doi.org/10.1007/s11899-009-0011-8

Masson, K., Rönnstrand, L., 2009. Oncogenic signaling from the hematopoietic growth factor receptors c-Kit and Flt3. Cell. Signal. 21, 1717–1726. https://doi.org/10.1016/j.cellsig.2009.06.002

Menendez, J.A., Lupu, R., 2017. Fatty acid synthase (FASN) as a therapeutic target in breast cancer. Expert Opin. Ther. Targets 21, 1001–1016. https://doi.org/10.1080/14728222.2017.1381087

Menendez, J.A., Lupu, R., 2007. Fatty acid synthase and the lipogenic phenotype in

cancer pathogenesis. Nat. Rev. Cancer 7, 763–777. https://doi.org/10.1038/nrc2222

Merino Salvador, M., Gómez de Cedrón, M., Moreno Rubio, J., Falagán Martínez, S., Sánchez Martínez, R., Casado, E., Ramírez de Molina, A., Sereno, M., 2017. Lipid metabolism and lung cancer. Crit. Rev. Oncol. Hematol. 112, 31–40. https://doi.org/10.1016/j.critrevonc.2017.02.001

Meyuhas, O., 2015. Ribosomal Protein S6 Phosphorylation: Four Decades of Research, in: International Review of Cell and Molecular Biology. Elsevier, pp. 41–73. https://doi.org/10.1016/bs.ircmb.2015.07.006

Mukhopadhyay, N.K., Price, D.J., Kyriakis, J.M., Pelech, S., Sanghera, J., Avruch, J., 1992. An array of insulin-activated, proline-directed serine/threonine protein kinases phosphorylate the p70 S6 kinase. J. Biol. Chem. 267, 3325–3335.

O'Donnell, M.R., Tallman, M.S., Abboud, C.N., Altman, J.K., Appelbaum, F.R., Arber, D.A., Bhatt, V., Bixby, D., Blum, W., Coutre, S.E., De Lima, M., Fathi, A.T., Fiorella, M., Foran, J.M., Gore, S.D., Hall, A.C., Kropf, P., Lancet, J., Maness, L.J., Marcucci, G., Martin, M.G., Moore, J.O., Olin, R., Peker, D., Pollyea, D.A., Pratz, K., Ravandi, F., Shami, P.J., Stone, R.M., Strickland, S.A., Wang, E.S., Wieduwilt, M., Gregory, K., Ogba, N., 2017. Acute Myeloid Leukemia, Version 3.2017, NCCN Clinical Practice Guidelines in Oncology. J. Natl. Compr. Cancer Netw. JNCCN 15, 926–957. https://doi.org/10.6004/jnccn.2017.0116

Oh, J.E., Jung, B.H., Park, J., Kang, S., Lee, H., 2020. Deciphering Fatty Acid Synthase Inhibition-Triggered Metabolic Flexibility in Prostate Cancer Cells through

Untargeted Metabolomics. Cells 9, 2447. https://doi.org/10.3390/cells9112447

Pandey, P.R., Liu, W., Xing, F., Fukuda, K., Watabe, K., 2012. Anti-cancer drugs targeting fatty acid synthase (FAS). Recent Patents Anticancer Drug Discov. 7, 185–197. https://doi.org/10.2174/157489212799972891

Papaemmanuil, E., Gerstung, M., Bullinger, L., Gaidzik, V.I., Paschka, P., Roberts, N.D., Potter, N.E., Heuser, M., Thol, F., Bolli, N., Gundem, G., Van Loo, P., Martincorena, I., Ganly, P., Mudie, L., McLaren, S., O' Meara, S., Raine, K., Jones, D.R., Teague, J.W., Butler, A.P., Greaves, M.F., Ganser, A., Döhner, K., Schlenk, R.F., Döhner, H., Campbell, P.J., 2016. Genomic Classification and Prognosis in Acute Myeloid Leukemia. N. Engl. J. Med. 374, 2209–2221. https://doi.org/10.1056/NEJMoa1516192

Pascale, R.M., Calvisi, D.F., Simile, M.M., Feo, C.F., Feo, F., 2020. The Warburg Effect 97 Years after Its Discovery. Cancers 12, E2819. https://doi.org/10.3390/cancers12102819

Pathania, S., Pentikäinen, O.T., Singh, P.K., 2021. A holistic view on c-Kit in cancer: Structure, signaling, pathophysiology and its inhibitors. Biochim. Biophys. Acta BBA - Rev. Cancer 1876, 188631. https://doi.org/10.1016/j.bbcan.2021.188631

Pathania, S., Rawal, R.K., 2020. An update on chemical classes targeting ERK1/2 for the management of cancer. Future Med. Chem. 12, 593–611. https://doi.org/10.4155/fmc-2019-0339

Patnaik, M.M., 2018. The importance of FLT3 mutational analysis in acute myeloid leukemia. Leuk. Lymphoma 59, 2273–2286. https://doi.org/10.1080/10428194.2017.1399312

Pollard, J.A., Alonzo, T.A., Gerbing, R.B., Ho, P.A., Zeng, R., Ravindranath, Y., Dahl, G., Lacayo, N.J., Becton, D., Chang, M., Weinstein, H.J., Hirsch, B., Raimondi, S.C., Heerema, N.A., Woods, W.G., Lange, B.J., Hurwitz, C., Arceci, R.J., Radich, J.P., Bernstein, I.D., Heinrich, M.C., Meshinchi, S., 2010. Prevalence and prognostic significance of KIT mutations in pediatric patients with core binding factor AML enrolled on serial pediatric cooperative trials for de novo AML. Blood 115, 2372–2379. https://doi.org/10.1182/blood-2009-09-241075

Raffel, S., Falcone, M., Kneisel, N., Hansson, J., Wang, W., Lutz, C., Bullinger, L., Poschet, G., Nonnenmacher, Y., Barnert, A., Bahr, C., Zeisberger, P., Przybylla, A., Sohn, M., Tönjes, M., Erez, A., Adler, L., Jensen, P., Scholl, C., Fröhling, S., Cocciardi, S., Wuchter, P., Thiede, C., Flörcken, A., Westermann, J., Ehninger, G., Lichter, P., Hiller, K., Hell, R., Herrmann, C., Ho, A.D., Krijgsveld, J., Radlwimmer, B., Trumpp, A., 2017. BCAT1 restricts αKG levels in AML stem cells leading to IDHmut-like DNA hypermethylation. Nature 551, 384–388. https://doi.org/10.1038/nature24294

Rapp, U.R., Goldsborough, M.D., Mark, G.E., Bonner, T.I., Groffen, J., Reynolds, F.H., Stephenson, J.R., 1983. Structure and biological activity of v-raf, a unique oncogene transduced by a retrovirus. Proc. Natl. Acad. Sci. U. S. A. 80, 4218–4222. https://doi.org/10.1073/pnas.80.14.4218

Rapp, U.R., Todaro, C., 1978. Generation of new mouse sarcoma viruses in cell culture. Science 201, 821–824. https://doi.org/10.1126/science.210501

Ray, L.B., Sturgill, T.W., 1988. Characterization of insulin-stimulated microtubule-associated protein kinase. Rapid isolation and stabilization of a novel serine/threonine kinase from 3T3-L1 cells. J. Biol. Chem. 263, 12721–12727.

Recher, C., Dos Santos, C., Demur, C., Bardet, V., Prade-Houdellier, N., Laurent, G., Payrastre, B., 2006. Lyn Kinase Is Constitutively Activated, Controls the mTOR/p70S6K/4E-BP1 Pathway and Regulates Cell Proliferation in Acute Myeloid Leukemia. Blood 108, 1946. https://doi.org/10.1182/blood.V108.11.1946.1946

Roboz, G.J., 2011. Novel approaches to the treatment of acute myeloid leukemia. Hematol. Am. Soc. Hematol. Educ. Program 2011, 43–50. https://doi.org/10.1182/asheducation-2011.1.43

Röhrig, F., Schulze, A., 2016. The multifaceted roles of fatty acid synthesis in cancer. Nat. Rev. Cancer 16, 732–749. https://doi.org/10.1038/nrc.2016.89

Shafik, N.F., Ibraheem, D., Selim, M.M., Allam, R.M., Fathalla, L.A., 2022. The Prognostic Significance of c-KIT Mutations in Core Binding Factor Acute Myeloid Leukemia. Clin. Lymphoma Myeloma Leuk. 22, e363–e375. https://doi.org/10.1016/j.clml.2021.11.015

Sinha, C., Cunningham, L.C., Liu, P.P., 2015. Core binding factor AML: New prognostic categories and therapeutic opportunities. Semin. Hematol. 52,

215–222. https://doi.org/10.1053/j.seminhematol.2015.04.002

Smalley, K.S.M., Sondak, V.K., Weber, J.S., 2009. c-KIT signaling as the driving oncogenic event in sub-groups of melanomas. Histol. Histopathol. 24, 643–650. https://doi.org/10.14670/HH-24.643

Stuani, L., Riols, F., Millard, P., Sabatier, M., Batut, A., Saland, E., Viars, F., Tonini, L., Zaghdoudi, S., Linares, L.K., Portais, J.-C., Sarry, J.-E., Bertrand-Michel, J., 2018. Stable Isotope Labeling Highlights Enhanced Fatty Acid and Lipid Metabolism in Human Acute Myeloid Leukemia. Int. J. Mol. Sci. 19, 3325. https://doi.org/10.3390/ijms19113325

Sun, L., Yao, Y., Pan, G., Zhan, S., Shi, W., Lu, T., Yuan, J., Tian, K., Jiang, L., Song, S., Zhu, X., He, S., 2018. Small interfering RNA-mediated knockdown of fatty acid synthase attenuates the proliferation and metastasis of human gastric cancer cells via the mTOR/Gli1 signaling pathway. Oncol. Lett. 16, 594–602. https://doi.org/10.3892/ol.2018.8648

Sung, H., Ferlay, J., Siegel, R.L., Laversanne, M., Soerjomataram, I., Jemal, A., Bray, F., 2021. Global Cancer Statistics 2020: GLOBOCAN Estimates of Incidence and Mortality Worldwide for 36 Cancers in 185 Countries. CA. Cancer J. Clin. 71, 209–249. https://doi.org/10.3322/caac.21660

Swaminathan, M., Wang, E.S., 2020. Novel therapies for AML: a round-up for clinicians. Expert Rev. Clin. Pharmacol. 13, 1389–1400. https://doi.org/10.1080/17512433.2020.1850255

Swierczyński, J., Sledziński, T., 2012. [Metabolic and regulatory function of fatty acid

synthase]. Postepy Biochem. 58, 175–185.

Tao, T., Su, Q., Xu, S., Deng, J., Zhou, S., Zhuang, Y., Huang, Y., He, C., He, S., Peng, M., Hocher, B., Yang, X., 2019. Down-regulation of PKM2 decreases FASN expression in bladder cancer cells through AKT/mTOR/SREBP-1c axis. J. Cell. Physiol. 234, 3088–3104. https://doi.org/10.1002/jcp.27129

Teperino, R., Aberger, F., Esterbauer, H., Riobo, N., Pospisilik, J.A., 2014. Canonical and non-canonical Hedgehog signalling and the control of metabolism. Semin. Cell Dev. Biol. 0, 81–92. https://doi.org/10.1016/j.semcdb.2014.05.007

Turcotte, L.P., Raney, M.A., Todd, M.K., 2005. ERK1/2 inhibition prevents contraction-induced increase in plasma membrane FAT/CD36 content and FA uptake in rodent muscle. Acta Physiol. Scand. 184, 131–139. https://doi.org/10.1111/j.1365-201X.2005.01445.x

Van de Sande, T., Roskams, T., Lerut, E., Joniau, S., Van Poppel, H., Verhoeven, G., Swinnen, J.V., 2005. High-level expression of fatty acid synthase in human prostate cancer tissues is linked to activation and nuclear localization of Akt/PKB. J. Pathol. 206, 214–219. https://doi.org/10.1002/path.1760

Ventura, R., Mordec, K., Waszczuk, J., Wang, Z., Lai, J., Fridlib, M., Buckley, D., Kemble, G., Heuer, T.S., 2015. Inhibition of de novo Palmitate Synthesis by Fatty Acid Synthase Induces Apoptosis in Tumor Cells by Remodeling Cell Membranes, Inhibiting Signaling Pathways, and Reprogramming Gene Expression. EBioMedicine 2, 808–824. https://doi.org/10.1016/j.ebiom.2015.06.020

Vivanco, I., Sawyers, C.L., 2002. The phosphatidylinositol 3-Kinase AKT pathway in

human cancer. Nat. Rev. Cancer 2, 489–501. https://doi.org/10.1038/nrc839

Wandzioch, E., Edling, C.E., Palmer, R.H., Carlsson, L., Hallberg, B., 2004. Activation of the MAP kinase pathway by c-Kit is PI-3 kinase dependent in hematopoietic progenitor/stem cell lines. Blood 104, 51–57. https://doi.org/10.1182/blood-2003-07-2554

Wang, W., Zhao, X., Wang, H., Liang, Y., 2008. Increased fatty acid synthase as a potential therapeutic target in multiple myeloma. J. Zhejiang Univ. Sci. B 9, 441–447. https://doi.org/10.1631/jzus.B0740640

Wang, Y., Ding, Q., Yen, C.-J., Xia, W., Izzo, J.G., Lang, J.-Y., Li, C.-W., Hsu, J.L., Miller, S.A., Wang, X., Lee, D.-F., Hsu, J.-M., Huo, L., LaBaff, A.M., Liu, D.-P., Huang, T.-H., Lai, C.-C., Tsai, F.-J., Chang, W.-C., Chen, C.-H., Wu, T.-T., Buttar, N.S., Wang, K.K., Wu, Y., Wang, H., Ajani, J., Hung, M.-C., 2012. The Crosstalk of mTOR/S6K1 and Hedgehog pathways. Cancer Cell 21, 374–387. https://doi.org/10.1016/j.ccr.2011.12.028

Yi, Y.W., You, K.S., Park, J.-S., Lee, S.-G., Seong, Y.-S., 2021. Ribosomal Protein S6: A Potential Therapeutic Target against Cancer? Int. J. Mol. Sci. 23, 48. https://doi.org/10.3390/ijms23010048

Zaytseva, Y.Y., Rychahou, P.G., Le, A.-T., Scott, T.L., Flight, R.M., Kim, J.T., Harris, J., Liu, J., Wang, C., Morris, A.J., Sivakumaran, T.A., Fan, T., Moseley, H., Gao, T., Lee, E.Y., Weiss, H.L., Heuer, T.S., Kemble, G., Evers, M., 2018. Preclinical evaluation of novel fatty acid synthase inhibitors in primary colorectal cancer cells and a patient-derived xenograft model of colorectal cancer. Oncotarget 9,

24787–24800. https://doi.org/10.18632/oncotarget.25361

9 Acknowledgement

I would like to express my sincere gratitude to all the people who supported and accompanied me in this work. Many thanks to Prof. Manfred Jücker for giving me the opportunity to complete this project in his working group and also for the his continuous supervision of my study as well as his great care and encouragement. Many thanks to Dr. Maxim Kebenko for his great support and supervision in the whole procedure and for reviewing my thesis. I would like to thank Hannah Voß, Bente Katharina Siebels, Dr. Anna Worthmann, Prof. Dr. Jörg Heeren, Dr. Malte Kriegs and Konstantin Hoffer. Thank you all for the great collaboration in this project. Furthermore, I would like to thank Prof. Dr. Walter Fiedler for his suggestions during discussion and for reviewing my thesis. I would also like to thank the entire AG Jücker for the friendly working atmosphere. Last but not least, I would like to thank my family and friends. It is because of your help and support that I can overcome the difficulties and doubts one by one until the successful completion of my study.

10 CV

10.1 Personal information:

Ruimeng Zhuang

Hagenbeckstrasse50 22527 Hamburg

born on 24.02.1991 in Xuzhou, Jiangsu, China

ruimengzh@163.com

10.2 Education

Sept.2015 ~ Jul.2017

Medical School, Southeast University, Master student in Internal Medicine

Sept.2010 ~ Jul.2015

Medical School, Southeast University, Bachelor of Medicine in Clinical Medicine

10.3 Research and Professional Experience

Jun.2020 ~ Oct.2023

Doctoral thesis at the Center for Experimental Medicine, Institute for biochemistry and signal transduction in the working group by Prof. Dr. rer nat Manfred Jücker
Title: Functional role of fatty acid synthase for signal transduction in human acute myeloid leukemia cells

Jul.2015 ~ Oct.2016

Research thesis: Application of Chimeric Antigen Receptor T Cell

Main work: literature search,cell culture

11 Eidesstattliche Versicherung

Ich versichere ausdrücklich, dass ich die Arbeit selbständig und ohne fremde Hilfe verfasst, andere als die von mir angegebenen Quellen und Hilfsmittel nicht benutzt und die aus den benutzten Werken wörtlich oder inhaltlich entnommenen Stellen einzeln nach Ausgabe (Auflage und Jahr des Erscheinens), Band und Seite des benutzten Werkes kenntlich gemacht habe.

Ferner versichere ich, dass ich die Dissertation bisher nicht einem Fachvertreter an einer anderen Hochschule zur Überprüfung vorgelegt oder mich anderweitig um Zulassung zur Promotion beworben habe. Ich erkläre mich einverstanden, dass meine Dissertation vom Dekanat der Medizinischen Fakultät mit einer gängigen Software zur Erkennung von Plagiaten überprüft werden kann.

Unterschrift: ....

Declaration of an oath

I expressly assure that I have written the work independently and without the help of others, that I have not used any sources and aids other than those specified by me and that I have taken the passages taken from the works used, either verbatim or in terms of content, individually by edition (edition and year of publication), volume and page of the work used. Furthermore, I assure that I have not yet submitted the dissertation to a subject representative at another university for review or have otherwise applied for admission to a doctorate. I agree that my dissertation can be checked by the dean's office of the medical faculty using standard software for detecting plagiarism.

Signature: ....